Fluorescent Quantum Dot Labeling of Canine Transferrin Receptor with Biotin Ligase

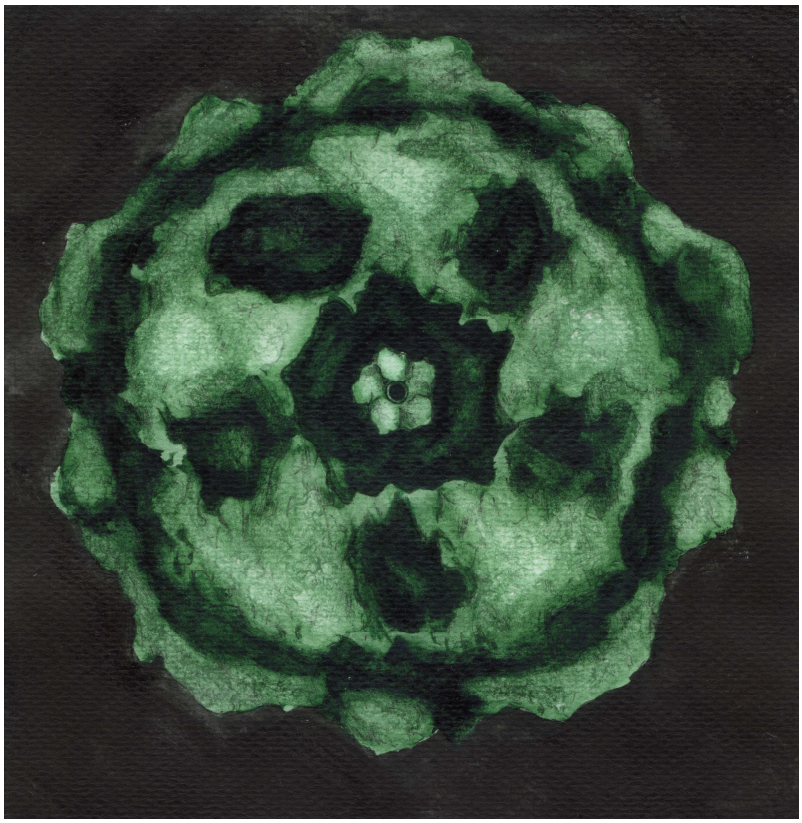

Pro gradu -tutkielma
Jyväskylän yliopisto
Bio- ja ympäristötieteiden laitos
Solubiologian osasto
Heinäkuu 2007
Outi Paloheimo

The great tragedy of science - the slaying
of a beautiful hypothesis by an ugly fact.

Thomas Huxley

Preface in Finnish

Tämä pro gradu- tutkielma tehtiin Jyväskylän yliopiston bio- ja ympäristötieteiden laitoksella molekyylibiologian osastolla vuosien 2006 - 2007 aikana. Haluan kiittää dosentti Maija Vihinen-Rantaa mahdollisuudesta osallistua tutkimukseen ja tutustua virusten mielenkiintoiseen maailmaan.

Haluan osoittaa suurkiitokset ohjaajilleni FM Teemu Ihalaiselle ja FM Einari Niskaselle hyvästä ohjauksesta ja antoisista yhteistyöhetkistä. Ilman heitä olisin jäänyt ilman paitsi jatkuvaa tukea, myös vapauksia ja itsensä toteuttamista sallivaa ohjausta. Teemun ja Einarin omistautuminen on ihailtavaa, kärsivällisyys käsittämätöntä ja innostus tarttuvaa.

Lisäksi haluaisin kiittää FM Juulia Jylhävää, FM Jenni Reimaria ja FM Johanna Rinnettä sekä muuta molekyylibiologian osaston henkilökuntaa lukuisista käytännön työtä koskevista neuvoista sekä lämpimän ja välittömän työilmapiirin luomisesta.

Jenni Karttusta, Sari Mäntystä ja Anne Vaaralaa kiitän monista tutkimukseen liittyvistä ja paljolti myös liittymättömistä ajatusten vaihtamisista ja keskusteluhetkistä.

Haluan osoittaa parhaimmat kiitokset rakkaalle perheelleni. Erityiskiitokset kuuluvat isälleni, joka on kannustanut ja tukenut minua koko opiskeluni ajan, sekä sisarelleni, joka on jaksanut väsymättä kuunnella ja vahvistaa minua. Kiitokset myös ystävilleni Essille, Marialle ja Marjutille, joiden kanssa olen aina voinut jakaa niin hyvät kuin huonotkin hetket.

Lopuksi minun täytyy vielä kiittää koiraani Giovannia, joka on graduntekijän paras ystävä.

Jyväskylän yliopisto **Pro gradu –tutkielman tiivistelmä**
Matemaattis-luonnontieteellinen tiedekunta

Tekijä: Outi Paloheimo
Tutkielman nimi: Koiran transferriinireseptorin leimaaminen fluoresoivilla kvanttipisteillä käyttäen biotiiniligaasia
English title: Fluorescent quantum dot labeling of canine transferrin receptor with biotin ligase
Päivämäärä: 30.07.2007 **Sivumäärä:** 58

Laitos: Bio- ja ympäristötieteiden laitos
Oppiaine: Solubiologia
Tutkielman ohjaajat: FM Teemu Ihalainen, FM Einari Niskanen, dosentti Maija Vihinen-Ranta

Tiivistelmä:

Transferriinireseptori (TfR) on solukalvon glykoproteiini, joka toimii osana sellulaarista rauta-aineenvaihduntaa. Rautaa sisältävä holotransferriini (Tf) sitoutuu solun pinnalla transferriinireseptoriin, joka kuljettaa sen solun sisään klatriinivälitteisen endosytoosin kautta. Endosomien matala pH indusoi konformaatiomuutoksia transferriinissa, joiden johdosta rauta vapautuu. Raudaton apotransferriini ja transferriinireseptori palaavat takaisin solukalvolle, jossa muutokset pH:ssa saavat aikaan apotransferriinin irtautumisen reseptorista.

Koiran parvoviruksella (CPV) ja transferriinilla on samankaltaisia ominaisuuksia. Infektoidakseen isäntäsolun myös CPV sitoutuu transferriinireseptoriin solun pinnalla. Endosomaalisten vesikkeleiden matala pH indusoi välttämättömiä konformaatiomuutoksia viruksen kapsidissa. Transferriinin kierto päättyy sen palatessa takaisin solukalvolle yhdessä transferriinireseptorin kanssa. Sen sijaan CPV kulkeutuu tumaan, jossa sen genomi replikoidaan. On yhä epäselvää, missä vaiheessa CPV vapautuu transferriinireseptorista. Yhtenä mielenkiinnon kohteena on tutkia, minne transferriinireseptorit, joihin CPV on sitoutunut, kulkeutuvat. Reseptorien seuraamiseksi tarvitaan menetelmä, jolla solun pinnan transferriinireseptoreita voidaan spesifisesti leimata.

Koiran transferriinireseptoreiden (cTfR) leimaamiseen ja fluoresenssimikroskooppikuvantamiseen käytettiin hyväksi fluoresoivia, streptavidiinikonjugoituja kvanttipisteitä (SA-QDs). Metodissa 15 aminohappoa pitkää vastaanottajapeptidiä (acceptor peptide, AP) ilmennetään reseptori-AP fuusioproteiinina (cTfR-AP). AP biotinyloidaan, ja se toimii ”kädensijana” streptavidiinikonjugoidulle kvanttipisteelle. cTfR-AP konstruktia ilmennettiin soluissa, joissa ei ole luonnostaan toiminnallista transferriinireseptoria (TRVb2-solut). *Escherichia coli*n biotiiniligaasia (BirA) käytettiin vastaanottajapeptidin biotinyloimiseen, minkä jälkeen streptavidiinikonjugoituja, fluoresoivia kvanttipisteitä käytettiin reseptorien tunnistamiseen.

Työssä selvitettiin, ilmentyykö cTfR-AP TRVb2-soluissa ja pystyvätkö transfektoidut solut välittämään CPV:n infektiota ja kulkeutumista soluun. Tutkimuksessa selvitettiin myös, pystyvätkö transfektoidut solut ottamaan sisäänsä streptavidiinia ja streptavidiinikonjugoituja kvanttipisteitä, ja onko sisäänotto riippuvaista reseptorien biotinyloimisesta.

Työssä saatiin selville, että cTfR-AP konstrukti ilmentyy TRVb2 soluissa, ja että cTfR-AP voidaan biotinyloida spesifisesti BirA:lla. Lisäksi saatiin selville, että solut, jotka ovat transfektoitu cTfR-AP fuusioproteiinilla ja biotinyloitu BirA:lla, pystyvät sitomaan streptavidiinia ja streptavidiinkonjugoituja kvanttipisteitä. Osoitettiin myös, että CPV pystyy infektoimaan cTfR-AP konstruktilla transfektoituja soluja biotinylaatiosta riippumatta.

Avainsanat: transferriinireseptori, koiran parvovirus, streptavidiinikonjugoidut kvanttipisteet, BirA

University of Jyväskylä
Faculty of Mathematics and Science

Abstract of Master´s Thesis

Author: Outi Paloheimo
Title of thesis: Fluorescent quantum dot labeling of canine transferrin receptor with biotin ligase
Finnish title: Koiran transferriinireseptorin leimaaminen fluoresoivilla kvanttipisteillä käyttäen biotiiniligaasia
Date: 30.07.2007 **Pages:** 58

Department: Department of Biological and Environmental Science
Chair: Cell Biology
Supervisors: M.Sc. Teemu Ihalainen, M.Sc. Einari Niskanen, Docent Maija Vihinen-Ranta

---

Abstract:

Transferrin receptor (TfR) is a membrane glycoprotein that mediates iron uptake into cells as a part of cellular iron metabolism. Binding of TfR to the iron loaded holotransferrin (Tf) takes place at the cell surface. After formation of the Tf-TfR complex, it is internalized via clathrin mediated endocytosis. Iron is released from Tf when it goes through conformational changes induced by acidic pH of the endosomes. Iron free Tf-TfR complex is transported back to the cell membrane where changes in pH cause dissociation of apo-transferrin from TfR.

There are some similarities in the behaviour of canine parvovirus (CPV) and Tf. To infect the host cell CPV also binds TfR at the cell surface. The low pH of endosomal vesicles induces essential conformational changes in the viral capsid. To complete the circle Tf is recycled back to the cell membrane but CPV is instead drifted into the nucleus to accomplish the viral entry.

It is still unclear when CPV is released from the TfR. One of the main interests is to see where CPV bound TfRs are going. To track receptors, specific labeling method of TfRs on the cell surface is needed.

For labeling and confocal fluorescent microscopy imaging of canine transferrin receptors (cTfRs) streptavidin-conjugated, fluorescent quantum dots (SA-QDs) were employed. In this method 15 amino acid long acceptor peptide (AP) is expressed as a TfR-AP fusion protein. AP is then biotinylated and used as a handle for SA-QD. Canine transferrin receptor construct containing AP (cTfR-AP) was expressed in TfR deficient cells (TRVb2 cells), biotin ligase from *Escherichia coli* (BirA) was used to biotinylate the acceptor peptide and fluorescent SA-QDs were attached to the biotinylated AP handles.

In this study it was tested whether TRVb2 cells are able to express the cTfR-AP construct and mediate endocytic entry and infection of the CPV. It was also clarified if cells transfected with the cTfR-AP could internalize streptavidin and SA-QDs and is this internalization dependent on prior biotinylation of the receptors.

It was shown that the cTfR-AP is expressed in TRVb2 cells and transfected receptor construct can be specifically biotinylated with the BirA. It was also shown that cells transfected with the cTfR-AP followed by biotinylation with BirA were are able to bind streptavidin and SA-QDs. It was demonstrated that CPV is able to infect cTfR-AP transfected TRVb2 cells regardless of biotinylation.

Keywords: transferrin receptor, canine parvovirus, streptavidin conjugated quantum dots, BirA

Table of Contents

ABBREVIATIONS

AP	acceptor peptide
AP-EGFR	epidermal growth factor receptor tagged with acceptor peptide
AP-GluR	glutamate receptor tagged with acceptor peptide
BCCP	biotin carboxyl carrier protein
BHS	biotin holoenzyme synthetase
biotin-DY-633	Dyomics biotin conjugated with Alexa Fluor-633
BirA	*Escherichia coli* biotin protein ligase
BPL	biotin protein ligase
BSA	bovine serum albumine
CdSe	cadmium selenide
CdTe	cadmium telluride
CHO	Chinese hamster ovary
CPV	canine parvovirus
cTfR	canine transferrin receptor
cTfR-ATC1	canine transferrin receptor construct tagged with acceptor peptide
DABCO	1, 4-diazabicyclo [2.2.2] octane
DCT-1	divalent cation transporter 1
DMEM	Dulbecco's modified Eagle's medium
DMT-1	divalent metal transporter 1
EDTA	ethylenediamine tetra acetic acid

FITC	fluorescein isothiocyanate
G418	aminoglycoside antibiotic Geneticin 418
GAM-AP	alkaline phosphatase conjugated to goat anti-mouse IgG
GAR-AP	alkaline phosphatase conjugated to goat anti-rabbit IgG
GFP	green fluorescence protein
HeLa	immortal cell line derived from Henrietta Lacks
InAs	indium arsenide
InP	indium phosphide
IRE	iron response element
IRE-BP	iron response element-binding protein
IRP	iron regulatory protein
LB	Luria-Bertani media
mRNA	messenger RNA
NRAMP2	natural resistance-associated macrophage protein 2
NS	non-sructural protein
PBS	phosphate buffered saline
PFA	paraformaldehyde
p.i.	post infection
PLA_2	phospholipase A2
PP_i	pyrophosphate, the anion $P_2O_7^{4-}$
QD	quantum dot
QD605	streptavidin conjugated cadmium selenide-zinc sulfide nanoparticle
R-G-D	arginine-glycine-aspartic acid motif

RNase A	ribonuclease A
SA	streptavidin
SA-QD	streptavidin conjugated quantum dot
SDS	sodium dodecyl sulfate
Tf	transferrin
Tf_{10}	multivalent transferrin
TfR	transferrin receptor
Tris	2-amino-2-hydroxymethyl-1, 3-propanediol
TRVb2	transferrin receptor variant b2
TRVb2+725 TfR	TRVb2 cells stably transfected with wild type feline transferrin receptor
wt-fTfR	wild type feline transferrin receptor
VP	(structural) virus protein
ZnS	zinc sulfide

1 INTRODUCTION

1.1 Canine parvovirus

Canine parvovirus (CPV) is a member of the autonomous parvoviruses and *Parvoviridae* family **(Fig. 1)**. *Parvoviridae* are a group of small nonenveloped viruses with linear, single-stranded DNA genomes of approximately 5 kb in length. The genome of CPV encodes four different proteins. VP-1 and VP-2 are structural proteins and NS-1 and NS-2 are nonstructural proteins (Reed, et al., 1988, for review see Parrish, 1990). VP-1 and VP-2 are translated from alternatively spliced messages. NS-1 and NS-2 are products of the same gene, but these proteins are read in different reading frames (Jongeneel, et al., 1986). In addition, CPV have structural VP-3 protein in full capsids. VP3 is formed by the posttranslational proteolytic cleavage of a peptide from the N terminus of VP-2 (for review see Cotmore and Tattersall, 1987). VP-2 can self-assemble into capsids (López de Turiso, et al., 1992, Saliki, et al., 1992) but VP-3 is present only in DNA containing capsids (Tsao, et al., 1991). DNA replication of CPV takes place in the nucleus and it is dependent on the active cell cycle (for review see Cotmore and Tattersall, 1987). Capsid symmetry of the CPV is icosahedral and with diameter of approximately 26 nm (Tsao, et al., 1991).

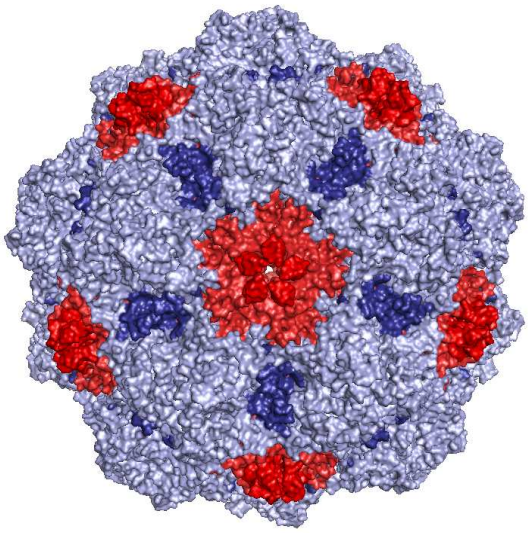

Figure 1. Surface Structure of the Canine Parvovirus. The surface of capsid consist twofold depressions (blue), regions of threefold protrusions (light blue) and fivelfold cylinder structures (red). Figure was made with The PyMOL Molecular Graphics System (DeLano, 2002), based on at 2.9 Å resolution structure analysis by Xie and Chapman, 1996. An unrefined 3.25 Å DNA-containing structure determination of the CPV capsid is reported by Tsao, et al., 1991.

1.1.1 Canine Parvovirus Capsid Assembly

CPV capsid is icosahedral with T = 1 symmetry (Tsao, et al., 1991). Virus capsid is assembled from 60 copies of overlapping symmetrical protein subunits, which mainly consist of VP-2 viral proteins, but also VP-1 and VP-3 proteins (for review see Cotmore and Tattersall, 1987, Tsao, et al., 1991). The structure of the CPV capsid is comprised of three different symmetry axes **(Fig. 2).** The surface of the capsid consist depressions at the twofold axes, protrusions at the threefold axes and cylinder structures at the fivelfold axes of symmetry. Fivefold axes of symmetry are surrounded by a circular depression, and this canyon-like structure is the possible site for receptor attachment. Hollow cylinders at the fivefold axes comprised of five eight-stranded antiparallel β-barrels (Tsao, et al., 1991). Each β-barrel has four extensive loops consisting of VP-protein. These loops connect the β-strands forming the most of the capsid outer surface and are important for the capsid assembly and morphology (Tsao, et al., 1991,

Hurtado, et al., 1996). Loops of β-barrels form protrusions at the threefold axes of symmetry. Between these threefold spikes there are depressions at the twofold axes of symmetry, called twofold dimples (Tsao, et al., 1991).

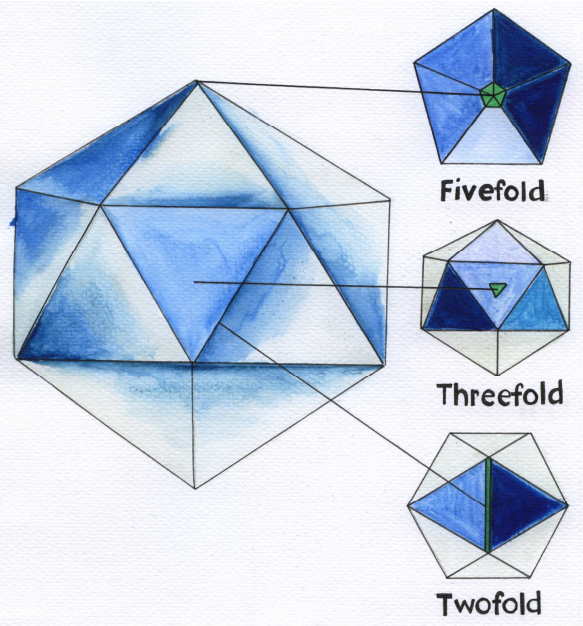

Figure 2. Icosahedral Symmetry of the Canine Parvovirus Capsid. An end-on view of twofold, threefold and fivefold rotational axes is shown at the right.

1.1.2 Entry and Infection Route of Canine Parvovirus

Entry of CPV takes place by endocytosis. To infect the host cell CPV binds to the transferrin receptor (TfR) at cell surface (Parker, et al., 2001). After binding to the receptor, virus is transported inside cell via dynamin dependent endocytic route with clathrin-coated vesicles. CPV capsids colocalize with endocytosed transferrin (Tf) (Xie and Chapman, 1996, Parker and Parrish, 2000). It is, however, still unclear when CPV is released from the receptor. After release from TfR, CPV passes through the cytoplasm by using microtubules into the nucleus via the nuclear pore (for review see Vihinen-Ranta, et al., 2004) where DNA replication, gene

expression and assembly of parvoviruses take place (Tattersall, 1972). Receptor mediated endocytosis of the recycling receptors requires acidic pH of the endosomes (for review see Pillay, et al., 2002). The low pH of endosomal vesicles induces conformational changes in the viral capsid. These changes are essential to accomplish the viral entry (Basak and Turner, 1992, Vihinen-Ranta, et al., 1998, Parker and Parrish, 2000). Transport of CPV to the perinuclear area is also dependent on the physiological temperature and on the intact microtubular network (Vihinen-Ranta, et al., 2000).

CPV infection route diverts from the clathrin-coated vesicles via early endosomes to the recycling endosomes. It is suggested that from the recycling endosomes CPV passes through the late endosomes to the lysosomes (Suikkanen, et al., 2002). There is some evidence indicating that CPV releases from lysosomes to the cytoplasm (Suikkanen, et al., 2003I) and that PLA_2 activity of the CPV capsid is needed on this process (Suikkanen, et al., 2003II). The N-terminal sequence of VP-1 protein of the CPV is buried within the capsid (Weichert, et al., 1998) and contains a phospholipase A_2 like domain (Zadori, et al., 2001). This domain can be exposed by urea treatment or at high temperature (Cotmore, et al., 1999). Furthermore, acidic pH can reveal PLA_2 activity of the CPV capsid and PLA_2 activity plays important role on the CPV entry process (Suikkanen, et al., 2003II). Although acidic pH in lysosomes expose the N-terminus of VP-1, there is evidence that CPV is released from vesicles to the cytoplasm in intact form (Vihinen-ranta, et al., 2000, Suikkanen, et al., 2003II). After released from the endocytic pathway CPV infection route diverts towards the nucleus. CPV transport into the nucleus is dependent on the nuclear localization signal of the N-terminus of VP-1, which locates near the PLA_2 domain (Vihinen-Ranta, et al., 1997). Potential carrier protein of CPV to the nucleus has been studied by microinjection of synthetic peptides into the cytoplasm of a canine fibroma cell line (A72 cells) (Binn, et al., 1980, Vihinen-Ranta, et al., 1997).

1.1.3 Host Range

Feline panleukopenia virus (FPV) and CPV DNA sequences are more than 99 % identical, but they still have different host ranges (Reed, et al., 1988, Parrish, et al., 1991, Truyen and Parrish, 1992). Both the CPV and the FPV are able to use transferrin receptor (TfR) to infect the cells. Binding of viruses is controlled by the differences between the feline and the canine TfR (Parker, et al., 2001), and regions of the CPV capsid are also important for determining the host range between the CPV and the FVP. Spikes on the threefold axes are important for antigenic features and the specific capsid conformation in this region is critical for the host specificity of CPV (Parker and Parrish, 1997). Feline cells can be infected both with the CPV and with the FPV, but only the CPV binds and infects the canine cells efficiently (Parker, et al., 2001).

1.2 Transferrin Receptor 1

The regulation of the intercellular iron concentration is essential for vertebrates (for review see Rouault and Klausner, 1996). Transferrin receptor (TfR) is a membrane glycoprotein that mediates iron uptake into cells and functions as a part of this regulation system (Trowbridge and Omary, 1981). Ingested iron binds to the transferrin protein (Tf) in blood circulation. Apotransferrin binds tightly into two Fe^{3+} ions. Iron loaded holotransferrin then binds to the TfR at the cell surface **(Fig. 3)**. Iron is transported by Tf to all tissue cells mainly from intestine and from liver. Except for erythrocytes there are TfRs at surface of all vertebrate cells and particularly on the surface of actively dividing cells (Lodish, et al., 2003).

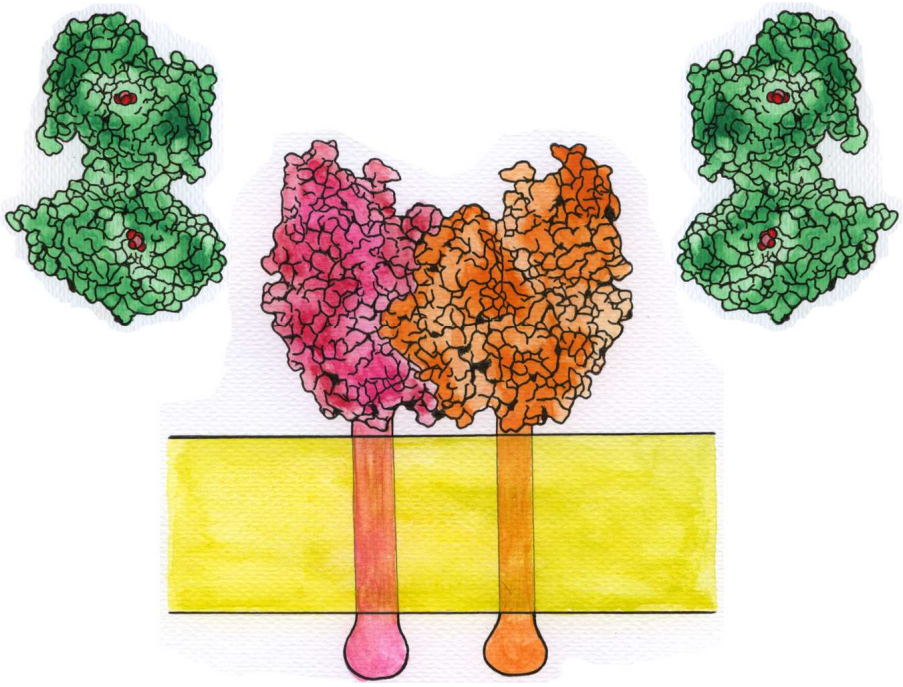

Figure 3. Binding of a Holotransferrin on the Outer Surface of Transferrin Receptor. Drawing is based on the space filling model of Hall, et al., 2002 (PDB: 1H76).

1.2.1 Structure of Transferrin Receptor 1

Twofold symmetric transferrin receptor 1 (TfR) dimer is a type II transmembrane protein composed of two disulphide-bonded subunits. Monomer of TfR has a short, N-terminal cytoplasmic region containing the internalization motif, a single transmembrane pass, and a large extracellular part. The extracellular part of the TfR or the ectodomain contains a binding site for transferrin (Tf). Ectodomain is soluble and bears a trypsin-sensitive site. 3D structure of the ectodomain of the human transferrin receptor expressed in Chinese hamster ovary (CHO) cells has been determined at 3.2 Å resolution (Lawrence, et al., 1999). Feline and canine TfR cDNA is approximately 80 % identical to the sequences of the human TfR (Parker, et al., 2001). TfR monomer with molecular weight of 90 kD has three distinct regions; a protease-like domain, an intermediate helical domain, and an apical domain. These domains organize in a way that the shape of TfR dimer resembling a butterfly. Each monomer of the TfR dimer binds one molecule of transferrin (Lawrence, et al., 1999).

The protease-like domain of the TfR contains seven-stranded β-sheet which is in the middle of the domain. The β-sheet is bounded by ten α-helices forming an extended loop. The apical domain of TfR reminds β-sandwich in which the two sheets are laid out with a helix leaving the open edge (Lawrence, et al., 1999). Changes in several residues of the apical domain affects binding of CPV into the cTfR and thus the apical domain is suggested to participate to the host-specificity of the CPV. Studies with purified canine TfRs verify the role of specific interactions between TfR and the CPV capsid in controlling viral host range (Palermo, et al., 2003, Palermo, et al., 2006). The TfR binds asymmetrically to the CPV, meaning that only one or few TfR molecules bind simultaneously. This either suggest that the CPV has some inherent asymmetry or then TfR binding can induce asymmetry (Hafenstein, et al., 2007).

The helical domain of the TfR is a four-helix bundle formed by a pair of parallel α-hairpins. The large loop-like insert contact the apical domain and the protease-like domain and appears to play an important role in the TfR dimerization. Certain parts of the protease-like and the helical domains participate in binding of Tf (Lawrence, et al., 1999). For instance R-G-D

sequence of the helical domain plays an important role in the binding of transferrin and this is supported by studies of site-directed mutagenesis (Dubljevic, et al., 1999).

1.2.2 Regulation of Synthesis of Transferrin Receptor 1

The iron response element-binding protein (IRE-BP) controls translation of ferritin mRNA and degradation of TfR mRNA. Synthesis of TfR is increased and synthesis of ferritin is inhibited when there is iron deficiency in cells. Effect of excess iron is opposite (Lodish, et al., 2003). Regulation of expression of the TfR is achieved through the 3' untranslated region of TfR mRNA (Müllner and Kühn, 1988). This stem-loop structure is termed the iron-regulatory element (IRE), which interacts with an IRE-binding protein (IRE-BP) (Rouault, et al., 1988, Koeller, et al., 1989). Similar stem-loop structure responsible for iron-dependent regulation exist in the 5' untranslated region of ferritin mRNA (Hentze, et al., 1987). At low intracellular iron concentrations IRE-BP binds to IRE in the 5' or 3' untranslated regions of ferritin or TfR mRNAs. At high iron concentrations IRE-BP undergoes a conformational change and cannot bind either mRNA **(Fig. 4)**. The dual control by IRE-BP precisely regulates the level of free iron ions within cells (Lodish, et al., 2003).

Regulation of TfR synthesis occurs via destabilization of TfR mRNAs (Müllner and Kühn, 1988), and the expression of ferritin is controlled at the level of translation initiation (Zahringer, et al., 1976). Repression of mRNA degradation leads to higher synthesis of TfR. This is because of the high-affinity interaction between IRE-BP and IRE in the TfR mRNA (Kühn and Hentze, 1992). In the TfR mRNA, stability depends on the five IREs (Casey, et al., 1988, Müllner and Kühn, 1988) and on the iron regulatory proteins (IRPs) **(Fig. 4)**. TfR mRNA degradation is inhibited, when IRPs bind to the IREs regions (Koeller, et al., 1989).

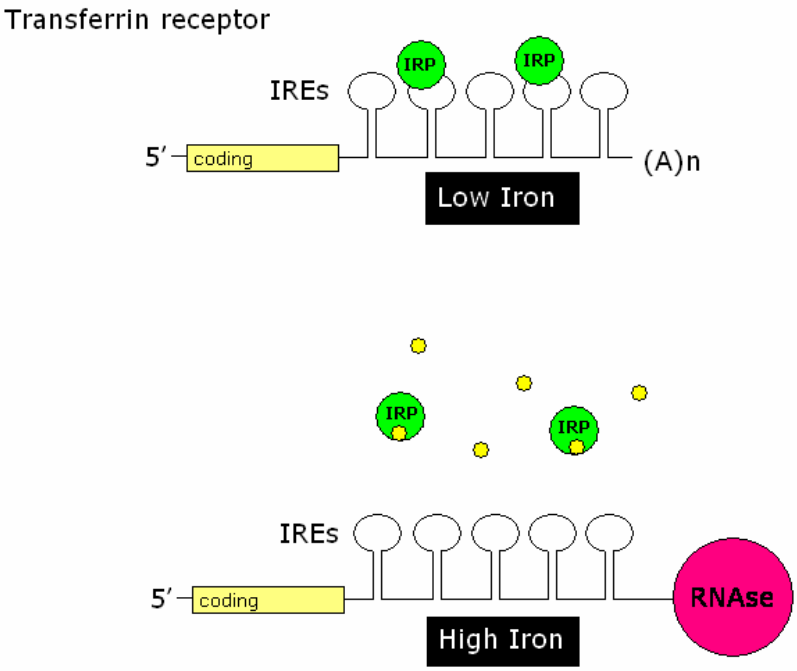

Figure 4. Regulation of mRNA by IRE-IRP Interaction. Synthesis of transferrin receptor (TfR) is regulated by a translational mechanism. In this mechanism the iron regulatory protein (IRP) is reversibly bound to the iron response element (IRE) of TfR mRNA. At low intracellular iron concentrations IRP binds to IRE in the 3' untranslated regions of TfR mRNA. At high iron concentrations IRPs cannot bind to the TfR mRNA. Picture is based on schematic by Harford, et al., 1994.

1.2.3 Recycling Route of Transferrin Receptor 1

Holotransferrin (Tf) interacts with the transferrin receptor (TfR) and iron loaded Tf-TfR-complex is internalized through clathrin mediated endocytosis. From clathrin-coated vesicles the complex ends up to the early endosomes (Lodish, et al., 2003). Iron is released from Tf when it goes through conformational change, caused by acidic pH of the endosomes (Cheng, et al., 2004). Apotransferrin remains bound in receptor but Fe^{3+} ion of the holotransferrin dissociate from complex when pH is lower than 6.0 (Lodish, et al., 2003). The Fe^{3+} ion is

released by acidification and reduction of Fe^{3+} to Fe^{2+} (for review see de Jong, et al., 1990). The divalent metal transporter 1 (DMT-1) is a key modulator of transferrin-bound iron homeostasis. DMT-1 is also known as natural resistance-associated macrophage protein 2 (NRAMP2) or as divalent cation transporter 1 (DCT-1). DMT-1 transports the Fe^{2+} to the cytoplasm (for review see Andrews, 1999). Iron free Tf-TfR-complex is transported back to the cell membrane. At the cell membrane higher pH induces the release of apo-transferrin from the receptor (Cheng, et al., 2004). Recycling TfR is able to bind a new pair of holotransferrin. Apotransferrin passes through blood circulation to the liver or to the intestine to be reloaded with iron (Lodish, et al., 2003).

There is evidence that binding of the CPV to the TfR changes its recycling route in cells by directing receptor towards the lysosomes. Redirecting of the TfR-CPV complexes to the lysosomes is suggested to be result of CPV-mediated clustering of the receptors (Suikkanen, et al., 2002). Recycling of the TfR usually completes when it is transported back to the plasma membrane in the recycling endosomes (Mayor, et al., 1993). However, when the CPV binds to the TfR, receptor can still be present while CPV is released to the cytoplasm. It is demonstrated that CPV and TfR colocalize together even after 10 hours from the beginning of virus entry (Suikkanen, et al., 2003I).

1.3 Biotin Ligase

1.3.1 Biotin and *Escherichia coli* BirA

Biotin is a vitamin H, an essential coenzyme and required by all forms of life. It is synthesized by plants, most bacteria and some fungi. Biotin is biologically active only when it is bound to protein. Intracellular biotin is covalently attached to the metabolic enzymes biotin carboxylases and decarboxylases. These enzymes are essential in gluconeogenesis, lipogenesis, amino acid degradation, and energy transduction. Carboxylases and decarboxylases catalyze the transfer of CO_2 to and between metabolites using biotin as a carrier of carboxyl (for review see Samols, et al., 1988). Biotin protein ligase (BPL) is the enzyme responsible for attaching biotin to the carboxylases and to the decarboxylases (Lane, et al, 1964, Eisenberg, et al., 1982). BPL is also known as holocarboxylase synthetase or as biotin holoenzyme synthetase (BHS) (for review see Chapman-Smith and Cronan, 1999, Chapman-Smith, et al., 2001). The carboxyl group of the biotin forms an amide linkage between the ε-amino groups of a specific lysine residue of the carboxylase protein. This two step reaction is catalysed by BPL (Lane, et al, 1964, Cronan, 1990). The best characterized BPL is the BirA of *E.coli*. It is a multifunctional protein and acts also in DNA binding repression of biotin (Campbell, et al., 1980).

1.3.2 Structure of BirA

BirA is a monomeric protein with molecular weight of 35.5 kDa. The three-dimensional structure of the BirA has been determined at 2.3 Å resolution by X-ray crystallography. It is an asymmetric protein with three distinct domains; the N-terminal DNA binding domain, the central domain, and the C-terminal domain (Wilson, et al., 1992). The N-terminal domain of the BirA is consisting of three α-helices packed against two strands of antiparallel β-sheet, forming a helix-turn-helix structural module. There is a slight interaction between the N-

terminal and the central domains in the apo-repressor structure (Wilson, et al., 1992). Binding of biotinyl-5´-AMP to the central domain increases the affinity of the N-terminal domain for DNA. This is indicative for a functional interaction between these two domains (Eisenberg, et al., 1982). The deletion of the N-terminal domain has damaging effects on binding of both biotin and biotinyl-5´-AMP to the protein. The N-terminal domain deletion also abolishes the DNA binding function of the BirA (Xu and Beckett, 1996).

The central domain of the BirA consists of five α-helices and a seven-stranded β-sheet. The central domain contains the residues that contact biotin in the crystal structure (Wilson, et al., 1992). Therefore the central domain is essential for the catalytic activity of the BirA enzyme and its interaction with ATP and the protein substrate (Chapman-Smith, et al., 2001). The central domain has considerable sequence homology with the eukaryotic biotin protein ligases (Tissot, et al., 1997). The central domain is required for the synthesis of biotinyl-5´-AMP. Central domain also mediates transfer of biotin from the adenylate to the lysine residue of the biotin carboxyl carrier protein (BCCP) of acetyl-CoA carboxylase. The adenylate functions as an activated intermediate in the biotin transfer reaction and as a positive allosteric effector for the site-spesific DNA-binding (Wilson, et al., 1992).

The C-terminal domain of the BirA is comprised of two three-stranded antiparallel β-sheet that cross each other forming a sandwich. One end of the biotin repressor is capped with this β-sheet sandwich structure (Wilson, et al., 1992). The C-terminal domain is also essential for the catalytic activity of the enzyme. The C-terminal domain is suggested to participate in to the interaction of ATP and the protein substrate BCCP (Chapman-Smith, et al., 2001).

1.3.3 Biotinylation Reaction

Biotinylation is one of the widely used means to label proteins. Biotinylated proteins can be easily detected with avidin or streptavidin, because they bind biotin with extremely high affinity (for review see Diamandis and Christopoulos, 1991). Reactions catalysed by BPL and the functional interaction between BPL and its protein substrate are strictly spesific. Biotin-dependent enzymes are abundant in nature, even though biotinylation is a relatively rare modification (Cronan, 1990). The mechanism of the biotin ligase reaction is straightforward. In a two-step reaction the biotin is attached post-translationally by BPL (for review see Chapman-Smith and Cronan, 1999).

(1) biotin + ATP ↔ biotinyl-5´-AMP + PPi

(2) biotinyl-5´-AMP + apo-protein → biotinylated holo-protein + AMP

At the first step biotinyl-adenylate or biotinyl-5´-AMP is synthesized from the substrates biotin and ATP (for review see Chapman-Smith and Cronan, 1999). Kinetic measurements of the binding of biotin and ATP to BPL demonstrate the order where biotin is binding first (Xu, et al., 1995). The attack by an oxygen atom of the biotin carboxylate on ATP is catalyzed by BPL. In the first half reaction forms also pyrophosphate (PPi). A biotinyl-5´-AMP remains bound in the active site and is quite stable until the presence of the apo-form of the biotin accepting domain of a biotin-requiring protein. At the second step biotinyl-5´-AMP is transferred to a specific lysine residue on the carboxylase. The nucleophilic ϵ-amino group of the lysine forms an amide bond between biotin and the lysine side chain. Once the amide bond is formed, the biotin remains attached to the protein molecule with very high affinity (for review see Chapman-Smith and Cronan, 1999).

1.4 Fluorescent Quantum Dots

Fluorescent quantum dots (QDs) are semiconductor nanoparticles with very high brightness and photostability. The use of QDs for protein labeling has several advantages when compared to the organic and small molecule dyes. Size- and composition-tunable emission of QDs from visible to infrared wavelengths and narrow emission spectrum facilitates imaging of many QDs simultaneously. The intense fluorescence emission of QDs allows tracking single protein molecules and they are highly resistant to photobleaching. Stability against photobleaching makes possible to imaging and tracking of QDs over a long period of time (for review see Chan, et al., 2002, Dahan, et al., 2003). Biomolecules such as peptides, proteins and DNA can be attach with QDs and these bioconjugates are being used for recent research and for developing new biochemical assays (for review see Chan, et al., 2002).

1.4.1 Quantum Dot Labeling and BirA

Escherichia coli BirA enzyme can be used with quantum dots (QDs) for specify tracking the protein of interest **(Fig. 5)**. BirA biotinylates the acceptor peptide (AP) and biotinylation of this short 15-amino acid peptide allows binding of avidin or streptavidin to the biotin for visualizing proteins (Schatz, 1993, Beckett, et al., 1999). Cell surface protein can be fused to the AP and be biotinylated by using the BirA, ATP and biotin. Streptavidin-conjugated QD binds to the biotinylated protein allowing detection of membrane protein trafficking (Howarth, et al., 2005).

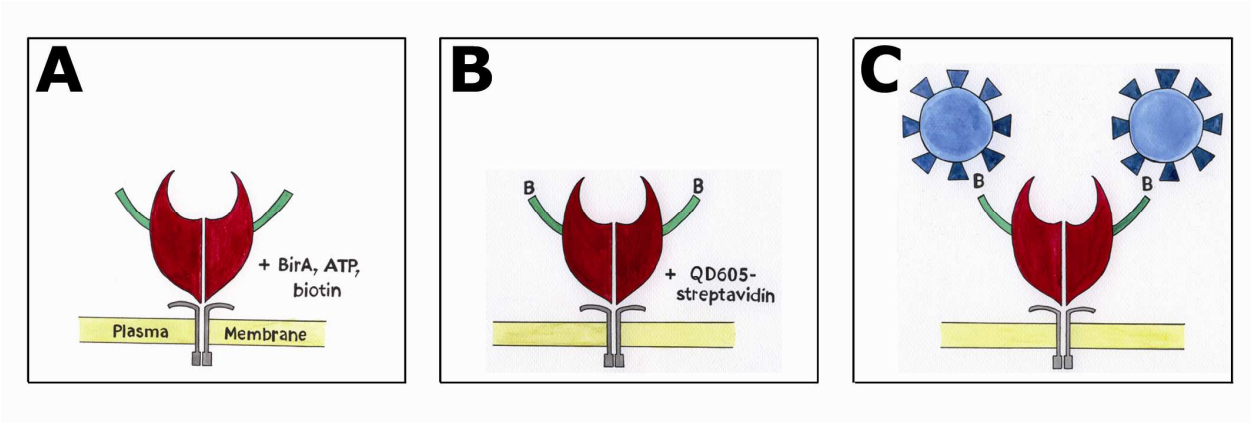

Figure 5. Method for Targeting Streptavidin Conjugated Quantum Dots (QD605-streptavidin) to the Canine Transferrin Receptor Tagged with Acceptor Peptide (cTfR-ATC1).
A) The acceptor peptide (AP, shown in green) is tagged with the canine transferrin receptor (cTfR).
B) Biotinylation of AP with *Escherichia coli* biotin ligase (BirA). BirA is added to the cell medium with ATP and biotin (B).
C) Streptavidin-conjugated QDs (QD605-streptavidin) are added to bind the biotinylated cTfR-ATC1.

It is suggested that AP unlikely disturbs the trafficking of a cell surface protein. This is because of the small size of the AP compared with other fluorescent probes, like green fluorescent protein (GFP) (Lisenbee, et al., 2003, Howarth, et al., 2005). Size of cadmium selenide-zinc sulfide nanoparticles (QD605, 6 nm) is slightly bigger than size of GFP (3 nm). However, for tracking the surface proteins, QDs are often conjugated for example with antibodies or with streptavidin **(Fig. 6).** The bigger size of different QD complexes can affect membrane protein trafficking and reduce their internalization to the cells (Jaiswal, et al., 2003, Howarth, et al., 2005, Huh, et al., 2003).

1.4.2 Synthesis and Optical Properties of Quantum Dots

Conjugated QDs are made from a nanometer scale crystal of semiconductor material, group II and VI elements such as cadmium selenide (CdSe) or cadmium telluride (CdTe) or group III and V elements such as indium arsenide (InAs) or indium phosphide (InP). Core material is coated with an additional semiconductor shell, which is usually from zinc sulfide (ZnS), and is further coated with a polymer shell or with other ligands **(Fig 6)**. Several polymers and ligands

allow the materials to be conjugated with biological molecules and to retain their optical properties. Also the nanocrystal size and shape can be controlled (Hines and Guyot-Sionnost, 1996, for review see Gao, et al., 2005).

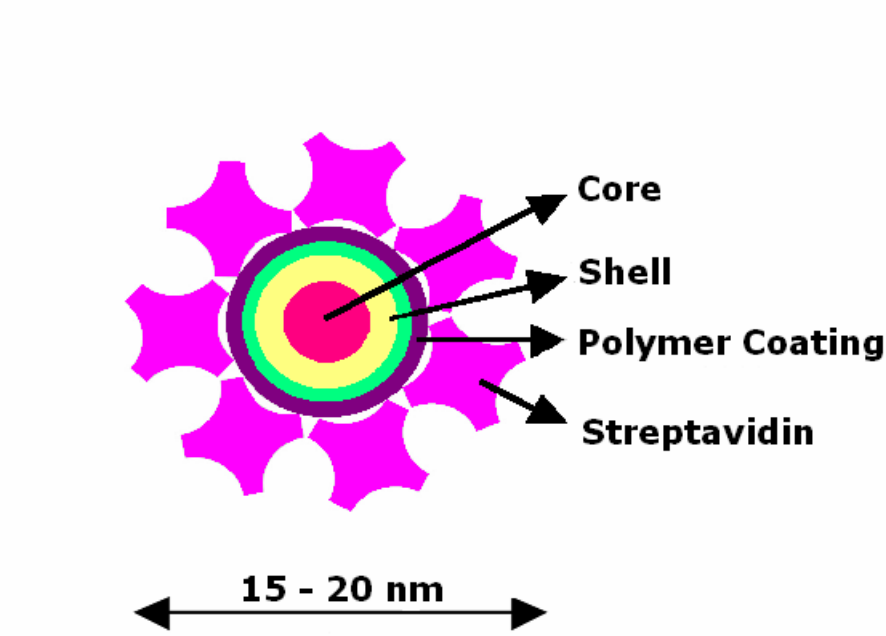

Figure 6. Structure of the Quantum Dot (QD) Bioconjugate. The layers are showing the distinct structural elements of the streptavidin conjugated QD (SA-QD). Picture is adaptation of the schematic by Watson, et al., 2003.

The optical properties of QDs are due to the semiconductor core. Core material of bioconjugated QDs effects to both the absorbance and emission properties. Bioconjugated QDs are activated by the absorption of a photon of light. Absorbed photon creates an electron-hole pair leading to emission of a lower-energy photon. In semiconductor material, for example in cadmium selenide, the energy of the emitted photon is determined by the size of the QD. This means that QDs with even small differences in their size emit different wavelengths of light (for review see Chan, et al., 2002).

Stokes shift is the difference between positions of maxima of the absorption and the maxima of the fluorescence of the same electronic transition. In other words, it is the difference between the position of the maximum absorbance and the maximum emission in the

electromagnetic spectrum. The Stokes shifts of QDs are large when compared to the typical fluorescent dyes, that have their optimal excitation wavelength is close to their emission peak. Depending on the excitation wavelength Stokes shifts of QDs can be as large as 300-400 nm (for review see Gao, et al., 2005). Typically for strongly absorbing organic dyes the Stokes shift is 30-50 nm (for review see Hemmilä, 1985).

The molar extinction coefficient ε of a chemical species at a given wavelength is a measure of how strongly the species absorbs light at that wavelength. Compared to the organic dyes QDs absorb more of the excitation light, and the molar extinction coefficients of QDs are approximately 50-500 $\times$ 10^4 $M^{-1}cm^{-1}$. It makes great difference compared to the molar extinction coefficient of the organic dyes, which are around 5-10 $\times$ 10^4 $M^{-1}cm^{-1}$.

The fluorescence quantum yield is the ratio of the number of photons emitted to the number of photons absorbed. For example, cadmium selenide QD with a zinc sulfide layer have quantum yield from 35 to 50 % (Hines and Guyot-Sionnost, 1996, Dabbousi, et al., 1997). Commercial QDs can have quantum yields up to 80 %, but the quantum yield can be reduced arising from conjugation to the biomolecules (for review see Watson, et al., 2003). Most of the organic dyes have relatively high quantum yields in their excitation and emission wavelength ranges (Panchuk-Voloshina, et al., 1999). For example, quantum yield to FITC is 85 %, to rhodamines it is approximately 70 % (for review see Hemmilä, 1985) and quantum yield of GFP is typically from 50 to 90 % upon a variation of GFP (Heim and Tsien, 1996, for review see Zimmer, 2002). Taken together, QD signals are still brighter than signals of the organic dyes (for review see Gao, et al., 2005).

2 AIM OF THE STUDY

2.1 The Spesific Aims of the Study

Aim of this study was to define whether TfR deficient TRVb2 cells (McGraw, et al., 1987) are able to express the canine transferrin receptor construct tagged with a 15-amino acid acceptor peptide (cTfR-ATC1) and are cells transfected with cTfR-ATC1 able to mediate endocytic entry and infection of the canine parvovirus (CPV). Focus was also on determination whether cTfR-ATC1 can be biotinylated site-spesific with *Escherichia coli* biotin ligase (BirA) and if the CPV is able to infect cTfR-ATC1 transfected cells regardless of biotinylation. Furthermore, the objective of this study was to clarify whether biotinylated cTfR-ATC1 is able to bind streptavidin (SA) and streptavidin-conjugated, fluorescent quantum dots (SA-QDs) and target biotinylated cTfR-ATC1 constructs bound to the SA or SA-QD and CPV in TRVb2 cells.

Methods used in this study consists mainly SA-QD labeling, techniques of immunofluorescence and fixed or live cell confocal microscopy imaging.

3 MATERIALS AND METHODS

3.1 Cell Culture

Two cell lines were used. Chinese hamster ovary (CHO) derived transferrin receptor variant b2 (TRVb2) cells that does not express detectable levels of functional hamster transferrin receptor (McGraw, et al., 1987) and TRVb2 cells stably transfected and expressing the wild type feline transferrin receptor (TRVb2+725 TfR) (Parker, et al., 2001). The cells were a gift from Professor Colin Parrish (Cornell University, Ithaca, NY). TRVb2 and TRVb2+725 TfR cells were maintained in Ham's F12-nutrient mixture (Gibco BPL, Paisley, UK) supplemented with 5 % fetal calf serum (Gibco BPL, Paisley, UK) and 1 % antibiotic mixture of penicillin and streptomycin (Gibco BPL, Paisley, UK). TRVb2+725 TfR cells growth media was also supplemented with selective antibiotic, 400 µg/ml Geneticin 418 (G418, Sigma Chemical Co., Germany). Cells were grown in monolayer in 75 cm^2 cell culture flasks (Sarstedt Inc., Newton, USA) at 37°C, in 5% CO_2 and passaged two times a week.

3.2 Bacterial Expression and Purification of BirA

His-tagged BirA was transformed into *E.coli* BL21 (AI) cells. A single colony from a fresh plate was picked and inoculated into 50 ml LB containing 0.2 % glucose and 4.9 µg/ml gentamycin at room temperature. Preculture was incubated at +37 °C for overnight (O/N). 450 ml of LB (1 % Bacto tryptone, 1 % NaCl, and 0.5 % Bacto yeast extract) was added into 50 ml preculture and supplemented with 0.2 % glucose and 4.9 µg/ml gentamycin. 500 ml culture was incubated at +37 °C until absorbance (600 nm) reached approximately 0.08. 0.4 % L-

arabinose was added to 500 ml culture for induced protein yield and cells were incubated at +28 °C for O/N.

The cells were pelleted and frozen at -70 °C for 10 minutes and they were thawed on ice. The cells were resuspended with 10 ml Binding Buffer (5 mM Imidazole, 0.5 M NaCl, and 20 mM Tris-HCl, pH 7.9) for 150 ml of culture. Triton-X-100 (Sigma) was added to final concentration of 0.1 % to enhance the cell lysis. The cells were sonicated on ice 3 times for 1 minute (1 second on and 1 second off with amplitude of 30 %) and centrifuged for 20 minutes at 15,000g and supernatant was filtered through Miracloth (Sigma).

1-2 ml of His-Bind resin (Novagen Inc., Germany) was washed with 10-20 ml of sterile water. Resin was activated with 5-10 ml of Charge Buffer (50 mM $NiSO_4$) and equilibrated with 3-6 ml of the Binding Buffer. The bacterial supernatant was allowed to bind to the resin at +4 °C for 1 h with gentle shaking. Mixture was centrifuged for 5 minutes at 500g and washed twice with 10-20 ml of the Binding Buffer.

The resin was further washed with 10-20 ml of the Wash Buffer (60 mM Imidazole, 0.5 M NaCl, and 20 mM Tris-HCl, pH 7.9) in a column. Proteins were eluted with 10 ml of the Elution Buffer (1 M Imidazole, 0.5 M NaCl, and 20 mM Tris-HCl, pH 7.9) and 1 ml fractions were collected and stored at -20°C. Column was regenerated by washing resin with the Strip Buffer (100 mM EDTA, 0.5 M NaCl, and 20 mM Tris-HCl, pH 7.9) and stored at +4°C in 5 ml of the Strip Buffer containing 7 µl NaN_3.

3.3 Expression Plasmid Induction and Purification of cTfR-ATC1

Modified canine transferrin receptor plasmid (cTfR-ATC1, constructed by Einari Niskanen) was transformed in *E.coli* JM109 cells by electroporation and plasmids were purified with DNA purification kit (Wizard Midiprep kits from Promega Corporation, USA).

3.4 Transfection with cTfR-ATC1

Transfection with cTfR-ATC1 construct was performed with TransIT-LT1 Transfection Reagent (Mirus) or FuGENE Reagent (Roche Applied Science). Following set ups were used for cells on 35-mm culture dishes (Sarstedt Inc., Newton, USA) with 2 ml of total volume of media.

5 µl of TransIT-LT1 was added to 250 µl of serum-free Dulbecco's modified Eagle's medium (DMEM) and incubated for 10-20 minutes at room temperature. 1 µg of DNA was added and incubation was continued for 20-30 minutes at room temperature.

6 µl of FuGENE was added to 94 µl of same DMEM-medium as described above and incubated for 5 minutes at room temperature. 1 µg of DNA was added and incubation was continued for 20 minutes at room temperature.

Media was removed from cells and replaced with fresh media. Transfection mixture was added to the cells and incubated at +37°C O/N. Media was replaced the next day with fresh media. After transfection cells were infected or labeled and living cells were also imaged the next day.

3.5 CPV Infection

Transfected or nontransfected TRVb2 cells were grown approximately in 80 % confluent on coverslips (diameter of 13 mm) and infected with CPV type 2 (CPV-d) (Parrish, 1991) particles containing DNA in growth media. 30 µl of virus suspension was added to each coverslip (1 µl of infective virus and 29 µl of growth media) and incubated at +37°C for 15 minutes. After incubation 2 ml growth media was added and incubation was continued at +37°C. After various times of post infection (p.i.) coverslips were rinsed with phosphate-buffered saline (PBS, 0.02 M sodium phosphate buffer with 0.15 M sodium chloride, pH 7.4) and fixed with 4% paraformaldehyde (PFA) for 20 minutes at room temperature, washed with PBS and stored in PBS at +4°C until immunolabeling.

3.6 Canine Transferrin Receptor Biotinylation

Transfected or nontransfected TRVb2 cells were washed in PBS (pH 7.4) with 5 mM $MgCl_2$ (PBS-Mg), and biotinylation was performed in PBS-Mg with 1 µM BirA, 10 µM biotin (Sigma), and 1 mM ATP (Promega, Madison, WI, USA) for 1-45 minutes at +37ºC.

The cells were washed with PBS-Mg at room temperature and incubated with 10 µg/ml streptavidin or various concentrations (5-50 nM) of streptavidin-QD605 (SA-QD) (QDs were from Molecular Probes and conjugated with streptavidin from Sigma by Teemu Ihalainen) in PBS-Mg supplemented with 1 % BSA (Roche, Mannheim, Germany) for 1-60 minutes at +37ºC. Biotinylation was also performed as time series and as concentration series. In time series cells were incubated with 1 µM BirA for 1-45 minutes at +37ºC and labeled after biotinylation with 10 µg/ml streptavidin for 60 minutes at +37ºC. In concentration series cells were incubated with BirA concentration varied from 100 to 1000 nM for 30 minutes at +37ºC and labeled after biotinylation with 30 nM SA-QD for 30 minutes at +37ºC.

After biotinylation and labeling the cells were washed with PBS-Mg and fixed in 4% PFA for 20 minutes at room temperature and washed with PBS. Cells labeled with SA-QD were washed with PBS for 20 minutes and embedded with Mowiol (Calbiochem) containing 30 mg/ml the antifading agent DABCO (Sigma). Cells labeled with SA were stored in PBS at +4°C after fixation until immunolabeling.

3.7 Labeling cTfR-ATC1 with Transferrin and Biotin

Transfected TRVb2 cells were biotinylated as described previously. After biotinylation cells were incubated with 250 µg/ml human transferrin conjugated with Alexa Fluor-546 (Molecular Probes) for 1 h at +37ºC or 40 µg/ml canine transferrin conjugated with Alexa Fluor-647 (a gift from Colin Parrish) for 15-60 minutes at +37ºC or with 2 µM Dyomics biotin conjugated with Alexa Fluor-633 (biotin-DY-633, a gift from PhD. Vesa P. Hytönen, ETH, Zürich, Switzerland) for 15 minutes at +37ºC. The cells were washed with PBS-Mg and fixed in 4% PFA for 20 minutes at room temperature, washed with PBS and embedded with Mowiol containing DABCO (30 mg/ml).

3.8 Immunolabeling

After incubation in permeabilization buffer (1 % BSA, 0.1 % Triton-X-100 and 0.01 % sodium azide in PBS) for 20 minutes, the coverslips were incubated with primary antibodies diluted in permeabilization buffer for 1 h at room temperature, and then rinsed with permeabilization buffer for 20 minutes, washed with PBS for 20 minutes and rinsed again with permeabilization buffer for 20 minutes before incubation with secondary antibody for 30 minutes at room temperature. Finally the coverslips were rinsed again with permeabilization

buffer for 20 minutes, and washed with PBS for 20 minutes at room temperature and embedded with Mowiol-DABCO (30 mg/ml).

3.9 Live Cell Imaging

In live cell imaging transfected TRVb2 cells were grown approximately in 80 % confluent on 50-mm culture dishes featuring a circular opening (10 mm) cut into the center of the attachment surface (MatTek Corporation, Ashland, USA). Cells were biotinylated as described previous. After biotinylation cells were washed with PBS-Mg and incubated with 40 nM SA-QD for 30 minutes at +37ºC and imaged in the growth media.

3.10 Antibodies

Antibodies used in this study.

Primary Antibodies

Antibody	Antibody produced in	Antibody source	Dilution used
Anti-NS-1	Mouse	a gift from Colin Parrish	1:200
A3B10/CPV capsid	Mouse	a gift from Colin Parrish	1:200
Anti-streptavidin	Rabbit	a gift from Professor Edward Bayer (The Weizmann Institute of Science, Rehovot, Israel)	1:1000

Secondary Antibodies

Antibody	Antigen	Antibody produced in	Antibody conjugated to	Antibody source	Dilution used
GAM-AP	Mouse IgG	Goat	Alexa Fluor-488	Molecular Probes	1:200
GAR-AP	Rabbit IgG	Goat	Alexa Fluor-488	Molecular Probes	1:200

3.11 Confocal Microscopy

In live cell imaging confocal microscopy was conducted with Zeiss LSM 510 (Axiovert 100M) Carl Zeiss with 63x objective (Plan Neofluar 63x/1.25 oil). Argon laser was used with excitation wavelength of 488 nm. Emission was collected between 545-585 nm. Used pixel size varied from 70 to 130 nm and pixel time (µs/pixel) varied from 0.64 to 2.56. Images sizes were 256x256, 512x512 or 1024x1024 pixels. Number of slices in stack images varied from 20 to 70, and slice thickness (µm/slice) varied from 0.48 to 0.55. Used averaging type was Line, ranged between 2 to 16.

Confocal microscopy of fixed cells was conducted with Olympus FluoView FV 1000 confocal laser scanning microscope with 60x objective (UPLSAPO 60x/1.35 oil). Used pixel size varied from 77 to 153 nm and pixel time (µs/pixel) varied from 2.0 to 4.0. Images sizes were 512x512, 640x640, 800x800, 1024x1024 or 2048x2048 pixels. Number of slices in stack images varied from 50 to 90, and slice size (µm/slice) varied from 0.13 to 0.15. Used averaging type was Line, varied from 2 to 20.

In imaging of CPV or SA-QD, Argon laser was used with excitation wavelength of 488 nm. Emission was detected between 500-600 nm. In SA, human transferrin or also SA-QD imaging, HeNe laser was used with excitation wavelength of 543. Emission wavelength ranged between 555-655 nm. In imaging of canine transferrin, HeNe laser was used with excitation wavelength of 633 nm. Emission was collected at 645-745 nm. When imaging simultaneously SA and CPV, Argon and HeNe laser was used with excitation wavelengths of 488 nm (CPV) and 543 nm (SA). Emission was detected between 500-530 nm (CPV) and between 555-625 nm (SA).When imaging simultaneously SA-QD and CPV, Argon and HeNe laser was used with excitation wavelengths of 488 nm (CPV) and 543 nm (SA-QD). Emission was collected between 500-530 nm (CPV) and between 555-655 nm (SA-QD).

4 RESULTS

4.1 Characterization of cTfR-ATC1 with CPV

To test whether the canine transferrin receptor construct (cTfR-ATC1) transfected cells can mediate CPV internalization, they were infected with CPV for 20 minutes, 1 h, 2 h, 4 h and for 24 h **(Fig. 7A)**. As a positive control TRVb2+725 TfR cells were also infected for 20 minutes, 1 h, 2 h, 4 h and for 24 h **(Fig. 7B)**. It has been shown that feline transferrin receptor can mediate both CPV and FPV entry and infection (Parker, et al., 2001). As a negative control untransfected TRVb2 cells were infected with CPV **(Fig. 7C)**. Viral capsids were detected at 20 minutes, 1 h, 2 h and 4 h post infection (p.i.). NS-1 protein could be detected in nucleus at 24 h p.i.

4.2 Characterization of cTfR-ATC1 with Transferrin

To test if cTfR-ATC1 is able to bind transferrin, TRVb2 cells were transfected with cTfR construct and labeled with human transferrin conjugated to Alexa Fluor-546 **(Fig. 8A)** or canine transferrin conjugated to Alexa Fluor-647. As a positive control TRVb2+725 TfR cells were also labeled with human transferrin **(Fig. 8B)** or with canine transferrin. Human transferrin was detected both transfected cells and cells with wild type feline transferrin receptor (wt-fTfR). Surprisingly, canine transferrin was not seen in cells transfected with cTfR-ATC1 or in cells with wt-fTfR (TRVb2+725 TfR cells).

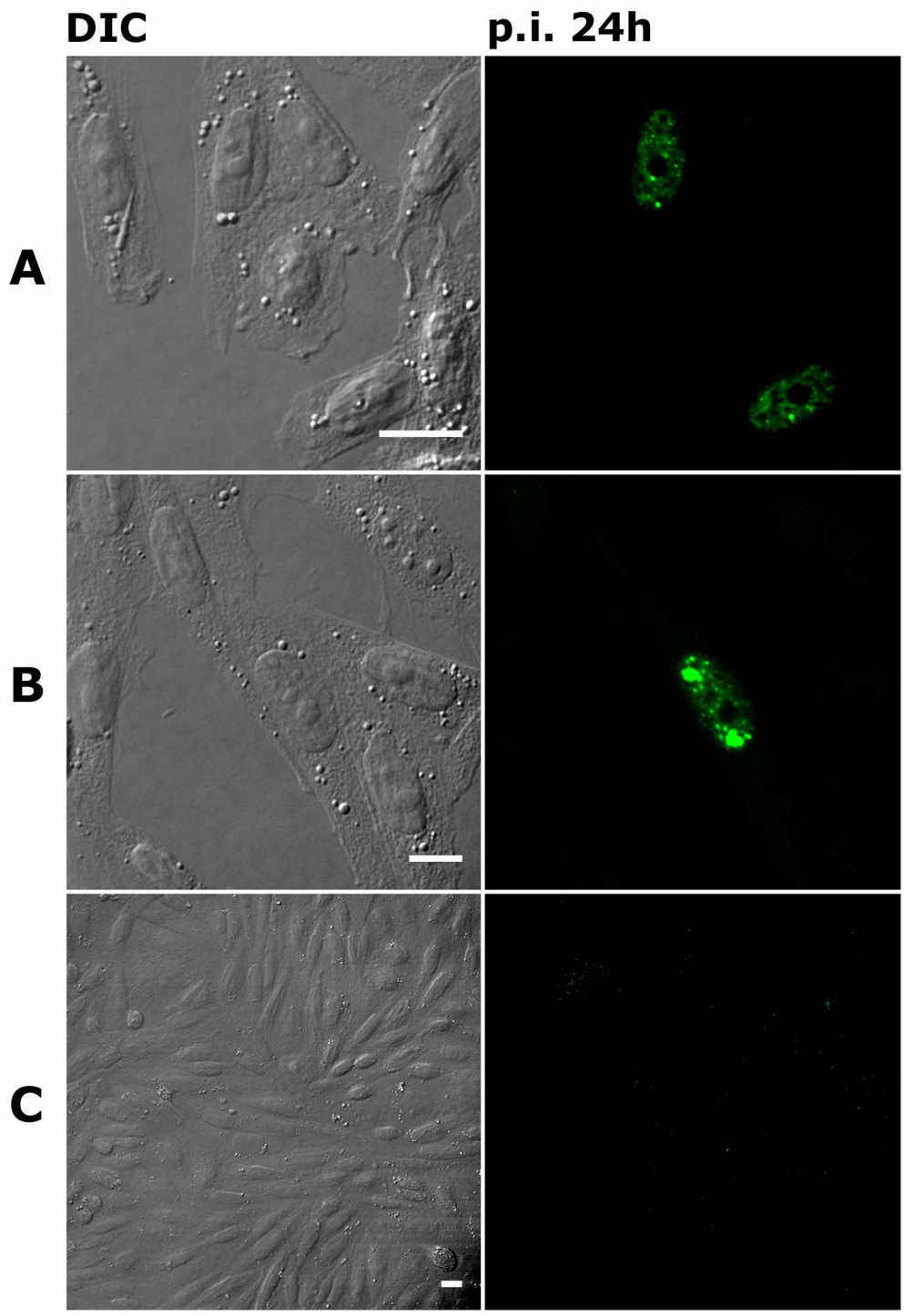

Figure 7. Receptor Construct Characterization with the Canine Parvovirus (CPV). All cells were infected with CPV, fixed 24 h post infection (p.i.) and immunolabeled with anti-NS-1 and GAM-AP-Alexa 488. **(A)** TRVb2 cells were transfected with cTfR-ATC1 receptor construct. NS-1 protein (green) is seen in the nucleus. **(B)** TRVb2+725 TfR cells expressing the wild type feline transferrin receptor showing the NS-1 protein in the nucleus. **(C)** In untransfected TRVb2 cells NS-1 protein can not be detected. Scale bars 10 µm.

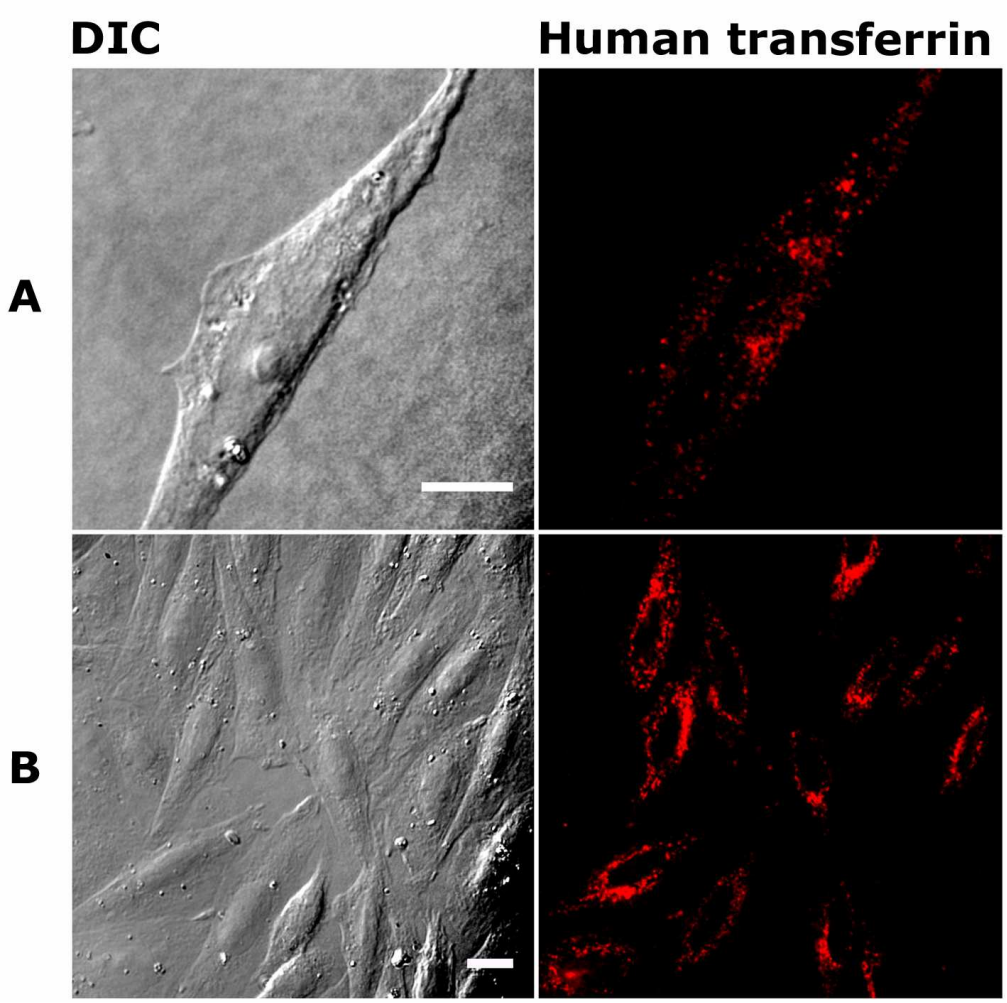

Figure 8. Receptor Construct Labeling with the Human Transferrin.
(A) TRVb2 cells were transfected with cTfR-ATC1 and labeled with human transferrin-Alexa Fluor 546 for 1 h at 37ºC. Human transferrin binding to the receptor construct is detected. **(B)** The same experiment with TRVb2+725 TfR cells expressing the wild type feline transferrin receptor. Binding of human transferrin to the wt-fTfR is seen. Scale bars 10 µm.

4.3 Site-Spesific Biotinylation of AP-Tagged Receptors

After TRVb2 cells were transfected with cTfR-ATC1 construct, BirA, ATP and biotin was added to the cell media. Biotinylated receptors were detected with biotin-DY-633 and streptavidin, or with streptavidin alone **(Fig. 9)** or with streptavidin-QD conjugate **(Fig. 10** and **Fig. 11).**

Streptavidin (SA) used in this study was conjugated to Alexa Fluor-555. In the presence of BirA, ATP and biotin, receptor labeling with SA was detected **(Fig. 9A)**. As a negative control, TRVb2 cells were transfected with cTfR-ATC1 but not treated with BirA **(Fig. 9B)**. SA was not seen in non-treated cells. Biotinylation was also detected with the biotin-DY-633 bound to SA. Both the biotin-DY-633 and SA was detected within BirA treated cells, but not in non-treated cells.

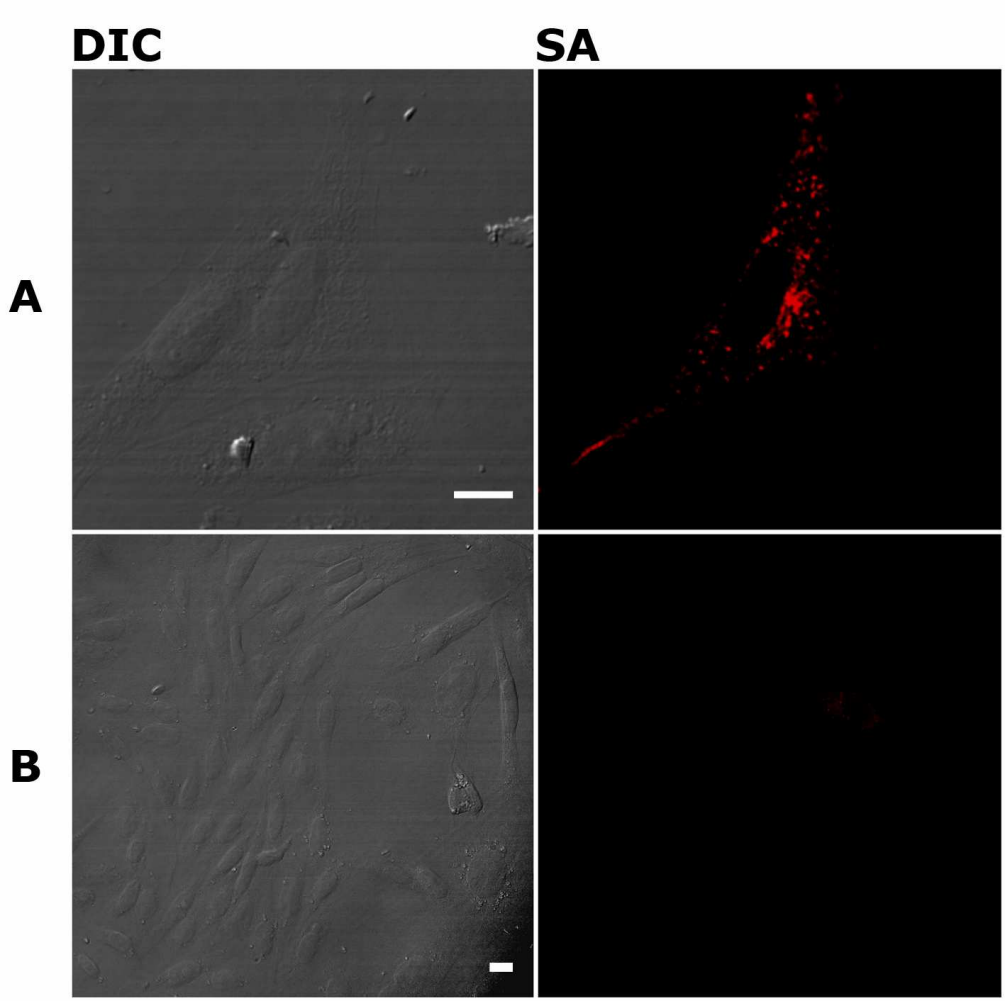

Figure 9. Site-Spesific Targeting of Streptavidin in TRVb2 Cells. All samples were transfected with cTfR-ATC1 and labeled with streptavidin-Alexa Fluor 555 for 30 minutes at 37ºC.
(A) Cells were treated with BirA for 30 minutes at 37ºC and SA (red) can be detected . **(B)** Cells were not biotinylated with BirA. Non-treated cells are not showing SA. Scale bars 10 µm.

Having verified the specificity of BirA for biotinylation of cTfR-ATC1 with SA, SA-QD labeling was performed. It was interesting to see could streptavidin-QD605 (SA-QD) be targeted to the receptor construct with similar specificity as SA. TRVb2 cells transfected with cTfR-ATC1 and treated with BirA showed strong receptor labeling with SA-QD **(Fig. 10C)**. For a first negative control untransfected cells were treated with BirA **(Fig. 10A)**. As a second negative control cells were transfected with receptor construct but not treated with BirA **(Fig. 10B)**. SA-QD was not detected in control cells. In live cell imaging TRVb2 cells were transfected and biotinylated same as described previous but imaged in the growth media immediately after incubation with SA-QD. Receptor labeling with SA-QD was detected in living cells, which were transfected with cTfR-ATC1 and biotinylated with BirA **(Fig. 11)**.

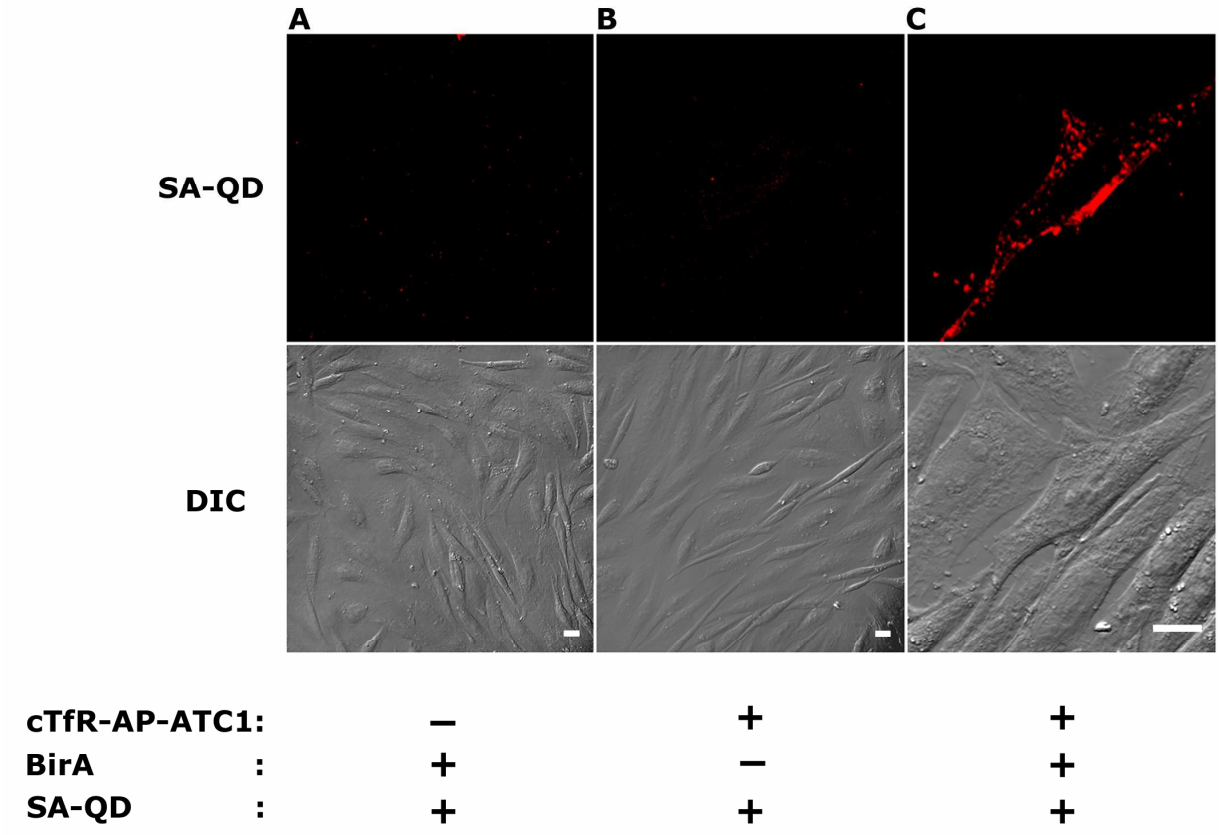

Figure 10. Site-Spesific Targeting of Streptavidin Conjugated Quantum Dots (SA-QDs) in TRVb2 Cells. All samples were labeled with SA-QD for 30 minutes at 37ºC.
(A) Untransfected cells were biotinylated with BirA for 30 minutes at 37ºC. **(B)** Cells were transfected with cTfR-ATC1 but not treated with BirA. **(C)** Cells were transfected with cTfR-ATC1 and incubated with BirA for 30 minutes at 37ºC. SA-QD is red. Scale bars 10 µm.

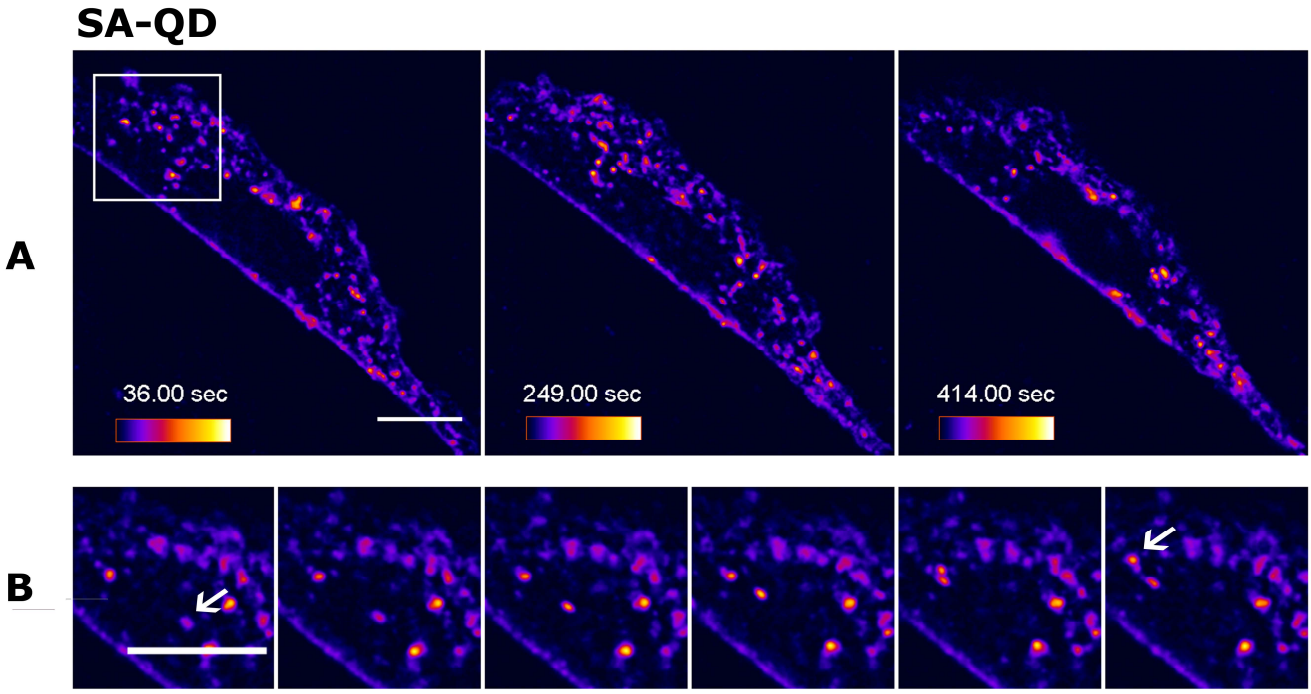

Figure 11. Live Cell Imaging and Streptavidin Conjugated Quantum Dot (SA-QD) Labeling of Receptors in TRVb2 Cells. Cells were transfected with cTfR-ATC1 and incubated with BirA for 30 minutes at 37ºC followed by SA-QD for 30 minutes at 37ºC. Cells were imaged in the growth media immediately after incubation with SA-QD.
(A) Cell was imaged over a period of several minutes. Images were taken 0.6 second frame rate.
(B) Blow-out image of detecting single receptor trafficking in the same cell. Images are shown with 1.8 seconds interval. Scale bars 10 µm.

4.4 Labeling Cells with SA or SA-QD with CPV

Localization of streptavidin (SA) with canine parvovirus (CPV) was studied with TRVb2 cells, which were transfected with canine transferrin receptor construct (cTfR-ATC1) and biotinylated and incubated together with SA and CPV **(Fig. 12A)**. Control cells were transfected but not treated with BirA **(Fig. 12B)**. CPV is seen both BirA treated cells and non-treated cells while SA is seen only in BirA treated cells. Streptavidin conjugated quantum dot (SA-QD) localization with CPV was reported by transfecting TRVb2 cells with cTfR-ATC1, followed by biotinylation and incubation together with SA-QD and CPV **(Fig. 13A)**. Control cells were transfected but not treated with BirA **(Fig. 13B)**. CPV is seen both BirA treated cells and non-treated cells while SA-QD is seen only in BirA treated cells.

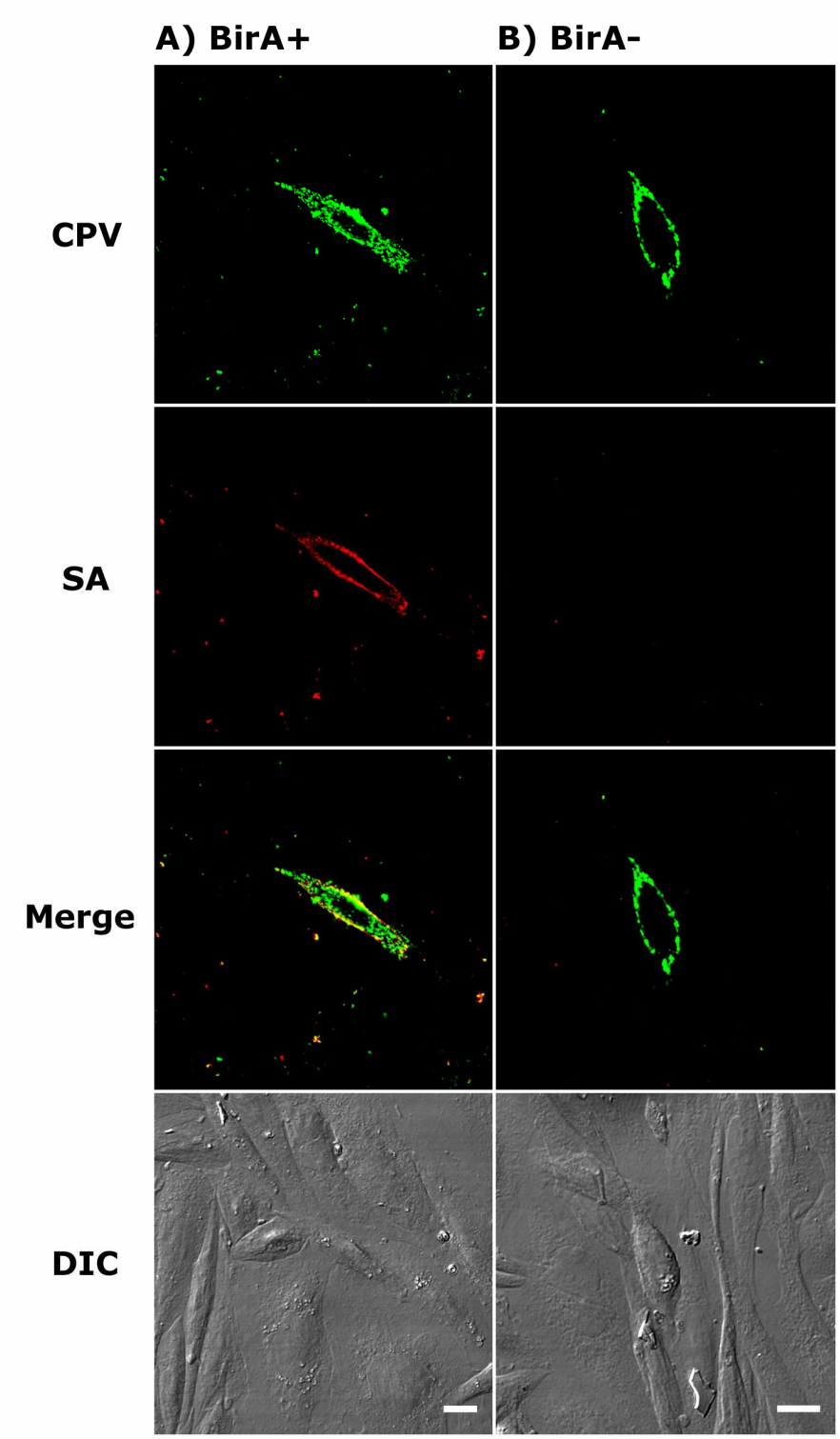

Figure 12. Localization of Streptavidin (SA) with the Canine Parvovirus (CPV) in TRVb2 cells. **(A)** Cells were transfected with cTfR-ATC1 followed by biotinylation with BirA for 30 minutes at 37ºC. Cells were then incubated simultaneously with CPV (green) and SA (red). **(B)** The same experiment, except the biotinylation. Scale bars 10 µm.

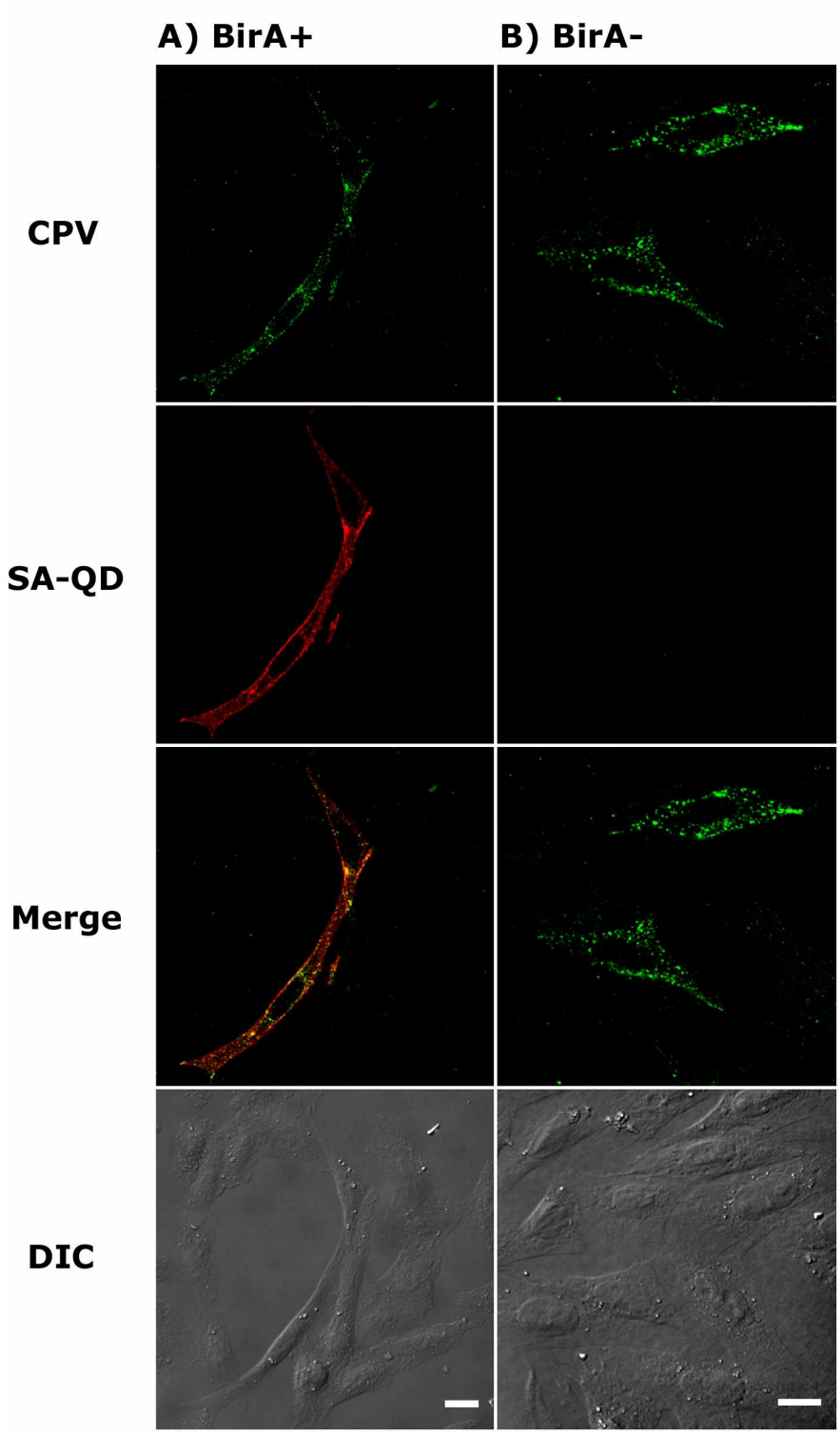

Figure 13. Localization of Streptavidin Conjugated Quantum Dots (SA-QDs) with the CPV in TRVb2 Cells. **(A)** Cells were transfected with cTfR-ATC1 followed by biotinylation with BirA for 30 minutes at 37ºC. Cells were then incubated simultaneously with CPV (green) and SA-QD (red). **(B)** The same experiment, except the biotinylation. Scale bars 10 µm.

4.5 Optimization of Labeling Procedure

Sensitivity of streptavidin conjugated quantum dot (SA-QD) in labeling of canine transferrin receptor tagged with acceptor peptide (cTfR-ATC1) was studied by performing concentration series with SA-QD concentration varied from 5 to 50 nM **(Fig. 14A)**. SA-QD started to show in cells after concentration reached 15 nM and SA-QD concentrations higher than 30 nM did not show significant improvement in the population of biotinylated receptors.

Sufficient concentration of BirA in biotinylation of cTfR-ATC1 was determined with concentration series, were concentration of BirA varied from 100 to 1000 nM **(Fig. 14B)**. SA-QD was used to detect biotinylation. SA-QD started to show in cells after BirA concentration reached 300 nM and concentrations higher than 600 nM did not show notable improvement in the efficacy of biotinylation.

Time rate of BirA receptor labeling on TRVb2 cells transfected with cTfR-ATC1 was determined with time series, were the biotinylation time varied from 1 to 45 minutes **(Fig. 14C)**. Streptavidin (SA) was used to detect biotinylation. Labeling could be detected after 1 minute of incubation with BirA and was maximal approximately after 10 minutes of incubation.

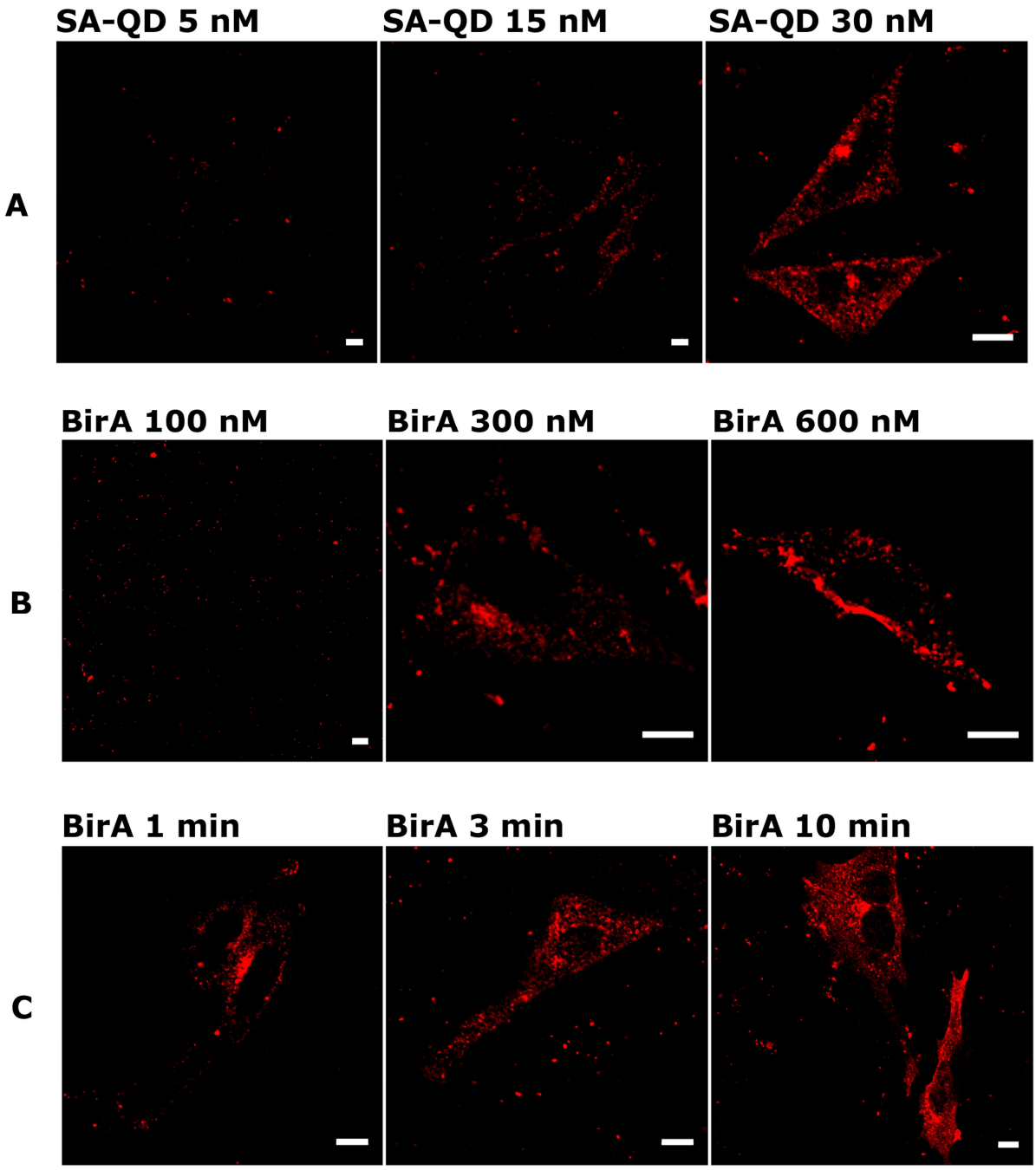

Figure 14. Sensitivity Testing of Biotinylation Method. All cells were transfected with cTfR-ATC1. **(A)** The effect of SA-QD concentration on receptor labeling. Cells were labeled with BirA for 30 minutes at 37ºC followed by various SA-QD (red) concentrations for 30 minutes at 37ºC. **(B)** The effect of BirA concentration on receptor labeling. Cells were labeled with various BirA concentrations for 30 minutes at 37ºC followed by SA-QD (red) for 30 minutes at 37ºC. **(C)** The time dependence of BirA on receptor labeling. Cells were labeled with BirA for various time points at 37ºC followed by streptavidin-Alexa Fluor 555 (red) for 60 minutes at 37ºC. Scale bars 10 µm.

5 DISCUSSION

The aim of this study was to determine if the TfR deficient cell line TRVb2 (McGraw, et al., 1987) is able to express the canine transferrin receptor construct tagged with a 15-amino acid acceptor peptide (cTfR-ATC1). It was tested whether cTfR-ATC1 transfected cells are able to internalize canine parvovirus (CPV) and if these cells can be infected with CPV. It was also studied whether cTfR-ATC1 is biotinylated with *E. coli* biotin ligase (BirA) and if CPV is able to infect those cells. Furthermore, it was determined if biotinylated cTfR-ATC1 is able to bind streptavidin (SA) and streptavidin-conjugated quantum dots (SA-QDs). Finally localization of SA or SA-QDs with CPV in biotinylated cTfR-ATC1 constructs was studied. Sensitivity of SA-QD labeling and biotinylation and rate of biotinylation of the cTfR-ATC1 was also investigated. Studies were mainly conducted with confocal microscopy by imaging both fixed and living cells.

5.1 Characterization of cTfR-ATC1 with CPV

Early stages of CPV infection have been elucidated quite well and new information has been gained during recent years. The CPV particles bound to the cell surface are clustered to the clathrin-coated vesicles and pits. Virus particles and Tf enter into cells via dynamin-dependent endocytosis (Parker and Parrish, 2000). Infection of CPV can be interrupted by endosome acidification preventing treatments. This suggests that CPV requires exposure to an acidic pH during viral entry to be able to accomplish the productive infection (Basak and Turner, 1992, Vihinen-ranta, et al., 1998, Parker and Parrish, 2000). CPV capsids trafficking towards the nuclear membrane can be inhibited by treating the cells with nocodazole. Nocodazole causes

depolymerization of microtubules demonstrating that intact microtubular network is needed to the CPV nuclear transport. Infective pathway of CPV is also inhibited by a reduction of the temperature (Vihinen-ranta, et al., 1998, Vihinen-Ranta, et al., 2000). However, from which endosomal organelle the CPV or its genome is released and an exact route from cytoplasm to the nucleus is still unclear.

CPV binds to the canine transferrin receptor (cTfR) at the cell surface (Parker, et al., 2001). Cycling of TfRs can follow the pathway of peripheral sorting endosomes or perinuclear recycling endosomes. Determined endocytic pathway of TfRs can depend on the ligands binding to the receptor (Daro, et al., 1996, Sheff, et al., 1999, Trischler, et al., 1999). Recycling route of TfR is suggested to change when multivalent form of Tf (Tf_{10}) is bound to the receptor (Marsh, et al., 1995). Moreover, binding of the ligands can cause clustering of TfRs rerouting them from the recycling pathway to the lysosomal pathway (Neutra, et al., 1985, Weissman, et al., 1986, Marsh, et al., 1995). It is hypothesized that binding of the CPV to the TfR changes its normal recycling route as well. This possibility is one motivation to study dynamics of TfRs.

TRVb2 cells were transfected with cTfR-ATC1 and it was shown that these cells are able to express cTfR-ATC1 by infecting cells with CPV. Viral capsids were detected in the cells at 20 minutes, 1 h, 2 h and 4 h post infection (p.i.) which verified that TRVb2 cells expressing of cTfR-ATC1 can mediate cell entry of the CPV. This demonstrated that acceptor peptide (AP) tagged with cTfR-ATC1 is unlikely to perturb CPV internalization. NS-1 protein could be detected in the nucleus at 24 h p.i. establishing that the CPV internalized via cTfR-ATC1 was able to lead to the productive infection. NS-1 is necessary for viral DNA replication and participates in the regulation of viral gene expression (Reed, et al., 1988). CPV did not infect untransfected TRVb2 cells demonstrating that the transfection and the expression of cTfR-ATC1 is needed for the viral entry.

5.2 Characterization of cTfR-ATC1 with Transferrin

Binding of cTfR-ATC1 to transferrin (Tf) was studied by transfecting TRVb2 cells with the construct followed by labeling with human transferrin conjugated to Alexa Fluor-546 or with canine transferrin conjugated to Alexa Fluor-647. It was also tested could TRVb2 cells with wild type feline transferrin receptor (TRVb2+725 TfR cells) bind human transferrin and canine transferrin. There is about 80 % identity between feline and canine TfR cDNA to the sequences of the human TfR (Parker, et al., 2001). It was shown that the human transferrin binds both to the cTfR-ATC1 transfected TRVb2 cells and to the TRVb2+725 TfR cells. Unexpectedly, canine transferrin was not detected in cells transfected with cTfR-ATC1 or in TRVb2+725 TfR cells. This could suggest that although acceptor peptide (AP) tagged to cTfR-ATC1 does not seem to effect internalization of CPV or human transferrin via receptor construct it can disturb binding of the canine transferrin. There is also a possibility that the canine transferrin used in this study was defective.

5.3 Site-Specific Biotinylation of AP-Tagged Receptors

As one aim of the study, it was determined if cTfR-ATC1 can be biotinylated site-spesific with BirA. It was shown that biotinylated cTfR-ATC1 constructs can be labeled with streptavidin-conjugated quantum dots (SA-QDs) or with streptavidin (SA), detected by immunofluorescence labeling and confocal microscopy. It has been demonstrated before that SA-QD binds to the biotinylated proteins bearing an AP by using method for the epidermal growth factor receptor (AP-EGFR) in HeLa cells and for glutamate receptors (AP-GluR1 and AP-GluR2) in neurons (Howarth, et al., 2005). In this study it was shown that BirA can specifically recognize cTfR-ATC1 at the cell surface. First, to study site-spesific biotinylation of cTfR-ATC1 by BirA, binding studies of SA and biotin-DY-633 or of SA alone were conducted. BirA and SA are not membrane-permeable, so intracellular proteins were not

labeled (Howarth, et al., 2005). TRVb2 cells transfected with cTfR-ATC1 followed by biotinylation showed binding and detectable colocalization of SA and biotin-DY-633. Binding of SA was also observed in transfected and BirA treated cells without biotin-DY-633. SA was not seen in TRVb2 cells which were transfected with cTfR-ATC1 but not treated with BirA demonstrating the specificity of streptavidin-biotin interaction.

After clarifying the site-specific targeting of SA to the biotinylated cTfR-ATC1, it was also studied whether SA-QD is able to attach to the BirA treated receptor construct using similar binding studies. Strong receptor labeling with SA-QD was detected in TRVb2 cells transfected with cTfR-ATC1 and followed by biotinylation with BirA. Similarly, SA-QD was not observed in cells which were treated with BirA but not transfected with cTfR-ATC1. SA-QD was not seen in cells which were transfected with receptor construct but not treated with BirA. Results demonstrate that cTfR-ATC1 is able to bind SA-QD and that interaction is dependent on prior biotinylation of receptors.

The transferrin receptor consist of a homodimer (Lawrence, et al., 1999) and in line with the wild type TfR, cTfR-ATC1 is able to bind two SA-QDs. Disadvantage to targeting cTfR-ATC1 constructs with SA-QD is possibility of QDs to cluster receptors. Clustering of the cTfR-ATC1 constructs could disrupt their recycling route and make detecting of a single receptor trafficking more difficult. One concern could also be the use of ATP with BirA and biotin in biotinylation method of cell surface receptors. It is conceivable that ATP added in the cells can effect on protein-protein interactions during biotinylation. ATP and its degradation products can also alter signaling pathways (for review see Rathbone, et al., 1999). However, it is shown that AP-tagged proteins can be biotinylated by BirA-biotin-AMP complex without addition of ATP into the medium (Howarth, et al., 2005).

In live cell imaging experiments, cTfR-ATC1 transfected TRVb2 cells were biotinylated with BirA and labeled with SA-QD. Intense receptor labeling was detected and confocal imaging demonstrated the stability of streptavidin-biotin interaction. Confocal microscopy studies of living cells also demonstrated the photostability of SA-QD, which allowed extended imaging.

In this study, live cell imaging with SA-QD was not compared to the organic dyes. However, it has been shown before that photostability of QDs allows imaging over much longer periods compared to the organic dyes (Howarth, et al., 2005).

Imaging of living cells was performed for periods of several minutes. It would be interesting to image SA-QD labeled receptors over longer periods, for example of hours to days. Long-term imaging could reveal more of the potential of SA-QD for tracking the cTfR-ATC1. SA-QD labeling of the cell surface receptors seems to a method that could be used for numbers of applications. It would also be interesting to study QD labeling with TRVb2 cells stably transfected with cTfR-ATC1, when variation of transfection effectiveness, altering down to transfection reagents, could be minimized. Expression levels of TRVb2 cells stably transfected with TfR-1 or TfR-2 are shown to stay relatively constant (Vogt, et al., 2003).

5.4 Labeling Cells with SA or SA-QDs with CPV

One of the interests in this study was to determine if biotinylated cTfR-ATC1 is able to bind streptavidin (SA) or streptavidin conjugated quantum dots (SA-QDs) and canine parvovirus (CPV) in TRVb2 cells and to study their localization. TRVb2 cells were transfected with cTfR-ATC1 followed by biotinylation and then incubation together with SA and CPV or together with SA-QD and CPV. Prospective colocalization was observed both between SA and CPV and between SA-QD and CPV. However, resolution of colocalization needs to be taken into account. Resolution of colocalization of the confocal microscopy used in the experiments with SA or SA-QD and CPV was approximately 200 nm, and is therefore limited by the size of the SA-QD (15-20 nm) and the size of the CPV (26-28 nm) (Tsao, et al., 1991, for review see Watson, et al., 2003, Howarth, et al., 2005). Despite hypothesized colocalization stayed below resolution, results assume that CPV and SA or SA-QD can bound separate sites in biotinylated cTfR-ATC1 construct. Results also suggest that labeling of cTfR-ATC1 with SA or SA-QD does not perturb viral entry of CPV. Internalization of SA and CPV

or SA-QD and CPV was also studied with cells which were transfected with receptor construct but not treated with BirA. As expected, CPV was detected both BirA treated cells and non-treated cells while SA and SA-QD were seen only in BirA treated cells. Results demonstrate that biotinylation of cTfR-ATC1 did not have detectable effect to the internalization of the CPV. Results also established previous results that binding of SA and SA-QD to the cTfR-ATC1 is dependent on prior biotinylation with BirA.

5.5 Optimization of Labeling Procedure

Sensitivity of streptavidin conjugated, fluorescent quantum dot (SA-QD) in labeling of canine transferrin receptor tagged with acceptor peptide (cTfR-ATC1) was studied by using SA-QD concentration series. SA-QD concentration varied from 5 to 50 nM. TRVb2 cells were transfected with cTfR-ATC1 followed by biotinylation with BirA. SA-QD was seen after concentration reached 15 nM and concentrations higher than 30 nM did not shown notable increment in the population of biotinylated receptors or improvement in levels of brightness. This demonstrated that labeling with SA-QD is a sensitive method for detecting biotinylated cTfR-ATC1 constructs.

Sensitivity of the biotinylation of the cTfR-ATC1 was studied with BirA concentration series. TRVb2 cells were transfected with cTfR-ATC1 and treated with BirA using concentration from 100 to 1000 nM followed by incubation with SA-QD. SA-QD was detected in cells after BirA concentration reached 300 nM. BirA concentrations higher than 600 nM did not displayed significant enhancement of the efficacy of biotinylation. This showed that BirA labeling with SA-QD is in addition to specific, also sensitive method for detecting and tracking cTfR-ATC1 constructs.

Rate of biotinylation of the cTfR-ATC1 was studied with BirA time series. TRVb2 cells were transfected with cTfR-ATC1, biotinylated and then labeled with streptavidin (SA). Treatment

time with BirA varied from 1 to 45 minutes. SA was observed after 1 minute incubation with BirA and no detectable increment in population of SA labeled receptors was seen after 10 minutes of incubation. Because biotinylation can be detected after 1 minute, method is potential to give more information and time resolution for studies of cTfR-ATC1 trafficking. Results also verified previous studies demonstrating that labeling with BirA is a rapid and applicable method for tracing dynamics of cell surface proteins (Howarth, et al., 2005).

5.6 Conclusions

Results of this study demonstrated that the canine transferrin receptor construct (cTfR-ATC1) is expressed in TRVb2 cells and that the canine parvovirus (CPV) is able to infect cells via cTfR-ATC1. It was shown that cTfR-ATC1 is specifically biotinylated with the BirA and construct is then able to bind streptavidin (SA) and streptavidin conjugated, fluorescent quantum dots (SA-QDs). It was also demonstrated that biotinylation of cTfR-ATC1 does not effect internalization or infection of the CPV. In the search for new labeling methods of receptors, interest has been directed towards fluorophores with improved photostability and brightness, long emission wavelength and large Stokes Shift. In this study it was shown that SA-QD resistance to photobleaching provides imaging of cTfR-ATC constructs over a relatively long period of time. Furthermore brightness of SA-QD facilitates tracking of single cTfR-ATC1 molecules. Focus in this study was also on entry and early stages of the CPV infection when it is bound to the cTfR. Information about trafficking of cTfR helps to understand CPV infection route as well. SA-QD labeling of receptors further able tracking of cTfRs. This method can be used to study dynamics of cell surface receptors, and mediation of the CPV bound to the cTfR. In addition, SA-QD labeling method used in this study provides extended imaging of the receptors at the cell surface. This method can also be potential to study releasing of the CPV from the cTfR.

REFERENCES

Andrews, N.C. 1999. The iron transporter DMT1. *Int. J Biochem. Cell Biol.* 31:991-994. Review.

Basak, S., and Turner, H., 1992. Infectious entry pathway for canine parvovirus. *Virology.* 186:368-376.

Beckett, D., Kovaleva, E., and Schatz, P.J. 1999. A minimal peptide substrate in biotin holoenzyme synthetase-catalyzed biotinylation. *Protein Sci.* 8:921-929.

Binn, L.N., Marchwicki, R.H., and Stephenson, E.H. 1980. Establishment of a canine cell line: derivation, characterization, and viral spectrum. *Am. J Vet. Res.* 41:855-860.

Campbell, A., Chang, R., Barker, D., and Ketner, G. 1980. Biotin regulatory (bir) mutations of *Escherichia coli*. *J Bacteriol.* 142:1025-1028.

Casey, J.L., Di Jeso, B., Rao, K., Rouault, T.A., Klausner, R.D., and Harford, J.B. 1988. The promoter region of the human transferrin receptor gene. *Ann. N Y Acad. Sci.* 526:54-64.

Chan, W.C., Maxwell, D.J., Gao, X., Bailey, R.E., Han, M., and Nie, S. 2002. Luminescent quantum dots for multiplexed biological detection and imaging. *Curr. Opin. Biotechnol.* 13:40-46. Review.

Chapman-Smith, A., and Cronan, J.E., Jr. 1999. In vivo enzymatic protein biotinylation. *Biomol.* 16:119-125. Review.

Chapman-Smith, A., Mulhern, T.D., Whelan, F., Cronan, J.E. Jr, and Wallace, J.C. 2001. The C-terminal domain of biotin protein ligase from *E. coli* is required for catalytic activity. *Protein Sci.* 10:2608-2617.

Cheng, Y., Zak, O., Aisen, P., Harrison, S.C., and Waltz, T. 2004. Structure of the human transferrin receptor-transferrin complex. *Cell.* 116:565-576.

Cotmore, S.F, and Tattersall, P. 1987. The autonomously replicating parvoviruses of vertebrates. *Adv. Virus Res.* 33:91-174. Review.

Cotmore, S.F., D'abramo, A.M., Jr., Ticknor, C.M., and Tattersall, P. 1999. Controlled conformational transitions in the MVM virion expose the VP1 N- terminus and viral genome without particle disassembly. *Virology.* 254:169-181.

Cronan, J.E., Jr. 1990. Biotination of proteins in vivo. A post-translational modification to label, purify, and study proteins. *J Biol. Chem.* 265:10327-10333.

Dabbousi, B.O., Rodriguez-Viejo, J., Mikulec, F.V., Heine, J.R., Mattoussi, H., Ober, R., Jensen, K.F., and Bawendi, M.G. 1997. (CdSe) ZnS core-shell quantum dots: Synthesis and characterization of a size series of highly luminescent nanocrystallites. *J Phys. Chem. B.* 101:9463-9475.

Dahan, M., Levi, S., Luccardini, C., Rostaing, P., Riveau, B., and Triller, A. 2003. Diffusion dynamics of glycine receptors revealed by single-quantum dot tracking. *Science.* 302:442-445.

Daro, E., van der Sluijs, P., Galli, T., and Mellman, I. 1996. Rab4 and cellubrevin define different early endosome populations on the pathway of transferrin receptor recycling. *Proc. Natl. Acad. Sci.* 93:9559-9564.

Diamandis, E.P., and Christopoulos, T.K. 1991. The biotin-(strept)avidin system: principles and applications in biotechnology. *Clin. Chem.* 37:625-636. Review.

Dubljevic, V., Sali, A., and Goding, J.W. 1999. A conserved RGD (Arg-Gly-Asp) motif in the transferrin receptor is required for binding to transferrin. *Biochem. J.* 341:11-14.

Eisenberg, M.A., Prakash, O., and Hsiung, S.C. 1982. Purification and properties of the biotin repressor. A bifunctional protein. *J Biol. Chem.* 257:15167-15173.

Gao, X., Yang, L., Petros, J.A., Marshall, F.F., Simons, J.W., and Nie, S. 2005. In vivo molecular and cellular imaging with quantum dots. *Curr. Opin. Biotechnol.* 16:63-72. Review.

Hafenstein, S., Palermo, L.M., Kostyuchenko, V.A., Xiao, C., Morais, M.C., Nelson, C.D., Bowman, V.D., Battisti, A.J., Chipman, P.R., Parrish, C.R., and Rossmann, M.G. 2007. Asymmetric binding of transferrin receptor to parvovirus capsids. *Proc. Natl. Acad. Sci.* 104:6585-6589.

Hall, D.R., Hadden, J.M., Leonard, G.A., Bailey, S., Neu, M., Winn, M., and Lindley, P.F. 2002. The crystal and molecular structures of diferric porcine and rabbit serum transferrins at resolutions of 2.15 and 2.60 Å, respectively. *Acta. Crystallogr. D Biol. Crystallogr.* 58:70-80.

Harford, J.B. 1994. Cellular iron homeostasis: a paradigm for mechanisms of posttranscriptional control of gene expression. *Prog. Liver Dis.* 12:47-62. Review.

Heim, R., and Tsien, R.Y. 1996. Engineering green fluorescent protein for improved brightness, longer wavelengths and fluorescence resonance energy transfer. *Curr. Biol.* 6:178-182.

Hemmilä, I. 1985. Fluoroimmunoassays and immunofluorometric assays. *Clin. Chem.* 31:359-370. Review.

Hentze, M.W., Caughman, S.W., Rouault, T.A., Barriocanal, J.G., Dancis, A., Harford, J.B., and Klausner, R.D. 1987. Identification of the iron-responsive element for the translational regulation of human ferritin mRNA. *Science.* 238:1570-1573.

Hines, M.A., and Guyot-Sionnest, P. 1996. Synthesis and characterization of strongly luminescing ZnS-capped CdSe nanocrystals. *J. Phys. Chem.* 100:468-471.

Howarth, M., Takao, K., Hayashi, Y., and Ting, A.Y. 2005. Targeting quantum dots to surface proteins in living cells with biotin ligase. *Proc. Natl. Acad. Sci. USA.*102:7583-7588.

Huh, W.K., Falvo, J.V., Gerke, L.C., Carroll, A.S., Howson, R.W., Weissman, J.S., and O'Shea, E.K. 2003. Global analysis of protein localization in budding yeast. *Nature.* 425:686-691.

Hurtado, A., Rueda, P., Nowicky, J., Sarraseca, J., and Casal, J.I. 1996. Identification of domains in canine parvovirus VP2 essential for the assembly of virus-like particles. *J Virol.* 70:5422-5429.

Jaiswal, J.K, Mattoussi H., Mauro, J.M., and Simon, S.M. 2003. Long-term multiple color imaging of live cells using quantum dot bioconjugates. *Nat. Biotechnol.* 21:47-51.

de Jong, G., van Dijk, J.P., and van Eijk, H.G. 1990. The biology of transferrin. *Clin. Chim. Acta.* 190:1-46. Review.

Jongeneel, C.V., Sahli, R., McMaster, G.K., and Hirt, B. 1986. A precise map of splice junctions in the mRNAs of minute virus of mice, an autonomous parvovirus. *J Virol.* 59:564-573.

Koeller, D.M., Casey, J.L., Hentze, M.W., Gerhardt, E.M., Chan, L.N., Klausner, R.D., and Harford, J.B. 1989. A cytosolic protein binds to structural elements within the iron regulatory region of the transferrin receptor mRNA. *Proc. Natl. Acad. Sci.* 86:3574-3578.

Kühn, L.C., and Hentze, M.W. 1992. Coordination of cellular iron metabolism by post-transcriptional gene regulation. *J Inorg. Biochem.* 47:183-195. Review.

Lane, M.D., Rominger, K.L., Young, D.L., and Lynen, F. 1964. The enzymatic synthesis of holocarboxylase from apocarboxylase and (+)-biotin. *J Biol. Chem.* 239:2865-2871.

Lawrence, C.M., Ray, S., Babyonyshev, M., Galluser, R., Borhani, D.W., and Harrison, S.C. 1999. Crystal structure of the ectodomain of human transferrin receptor. *Science.* 286:779-782.

Lisenbee, C.S., Karnik, S.K., and Trelease, R.N. 2003. Overexpression and mislocalization of a tail-anchored GFP redefines the identity of peroxisomal ER. *Traffic.* 4:491-501.

Lodish, H., Berk, A., Matsudaira, P., Kaiser, C.A., Krieger, M., Scott, M.P., Zipursky, L., and Darnell, J. 2003. "An iron-sensitive RNA-binding protein regulates mRNA translation and degradation". "The endocytic pathway delivers iron to cells without dissociation of receptor-transferrin complex in endosomes". In book Molecular Cell Biology. W.H. Freeman and Company, New York. Chapters 12:522-523 and 17:731-732.

Lopez de Turiso, J.A., Cortes, E., Martinez, C., Ruiz de Ybanez, R., Simarro, I., Vela, C., and Casal, I. 1992. Recombinant vaccine for canine parvovirus in dogs. *J Virol.* 66:2748-2753.

Marsh, E.W, Leopold, P.L., Jones, N.L., and Maxfield, F.R. 1995. Oligomerized transferrin receptors are selectively retained by a lumenal sorting signal in a long-lived endocytic recycling compartment. *J Cell Biol.* 129:1509-1522.

Mayor, S., Presley, J.F., and Maxfield, F.R. 1993. Sorting of membrane components from endosomes and subsequent recycling to the cell surface occurs by a bulk flow process. *J Cell Biol.* 121:1257-1269.

McGraw, T.E., Greenfield, L., and Maxfield, F.R. 1987. Functional expression of the human transferrin receptor cDNA in Chinese hamster ovary cells deficient in endogenous transferrin receptor. *J Cell Biol.* 105:207-214.

Müllner, E.W., and Kühn, L.C. 1988. A stem-loop in the 3' untranslated region mediates iron-dependent regulation of transferrin receptor mRNA stability in the cytoplasm. *Cell.* 53:815-825.

Neutra, M.R., Ciechanover, A., Owen, L.S., and Lodish, H.F. 1985. Intracellular transport of transferrin- and asialoorosomucoid-colloidal gold conjugates to lysosomes after receptor-mediated endocytosis. *J Histochem. Cytochem.* 33:1134-1144.

Panchuk-Voloshina, N., Haugland, R.P., Bishop-Stewart, J., Bhalgat, M.K., Millard, P.J., Mao, F., and Leung, W.Y. 1999. Alexa dyes, a series of new fluorescent dyes that yield exceptionally bright, photostable conjugates. *J Histochem. Cytochem.* 47:1179-1188.

Parker, J.S., and Parrish, C.R. 1997. Canine parvovirus host range is determined by the specific conformation of an additional region of the capsid. *J Virol.* 71:9214-9222.

Parker, J.S., and Parrish, C.R. 2000. Cellular uptake and infection by canine parvovirus involves rapid dynamin-regulated clathrin-mediated endocytosis, followed by slower intracellular trafficking. *J Virol.* 74:1919-1930.

Parker, J.S., Murphy, W.J., Wang, D., O'Brien, S.J., and Parrish, C.R. 2001. Canine and feline parvoviruses can use human or feline transferrin receptors to bind, enter, and infect cells. *J Virol.* 75:3896-3902.

Parrish, C.R. 1990. Emergence, natural history, and variation of canine, mink, and feline parvoviruses. *Adv. Virus Res.* 38:403-450. Review.

Parrish, C.R. 1991. Mapping specific functions in the capsid structure of canine parvovirus and feline panleukopenia virus using infectious plasmid clones. *Virology.* 183:195-205.

Parrish, C.R., Aquadro, C.F., Strassheim, M.L., Evermann, J.F., Sgro, J.Y., and Mohammed, H.O. 1991. Rapid antigenic-type replacement and DNA sequence evolution of canine parvovirus. *J Virol.* 65:6544-6552.

Palermo, L.M., Hueffer, K., and Parrish, C.R. 2003. Residues in the apical domain of the feline and canine transferrin receptors control host-specific binding and cell infection of canine and feline parvoviruses. *J Virol.* 77:8915-8923.

Palermo, L.M., Hafenstein, S.L., and Parrish, C.R. 2006. Purified feline and canine transferrin receptors reveal complex interactions with the capsids of canine and feline parvoviruses that correspond to their host ranges. *J Virol.* 80:8482-8492.

Pillay, C.S, Elliott, E., and Dennison, C. 2002. Endolysosomal proteolysis and its regulation. *Biochem. J.* 363:417-429. Review.

Rathbone, M.P., Middlemiss, P.J., Gysberg, J.W., Andrew, C., Herman, M.A., Reeds, J.K., Ciccarelli, R., Diiorio, P., and Caciagli, F. 1999. Trophic effects of purines in neurons and glial cells. *Prog. Neurobiol.* 59:663-690. Review.

Reed, A.P., Jones, E.V. and Miller, T.J. 1988. Nucleotide sequence and genome organization of canine parvovirus. *J Virol.* 62: 266-276.

Rouault, T.A., Hentze, M.W., Caughman, S.W., Harford, J.B., and Klausner, R.D. 1988. Binding of a cytosolic protein to the iron-responsive element of human ferritin messenger RNA. *Science.* 241:1207-1210.

Rouault, T.A., and Klausner, R.D. 1996. Iron-sulfur clusters as biosensors of oxidants and iron. *Trends Biochem. Sci.* 21:174-177. Review.

Saliki, J.T., Mizak, B., Flore, H.P., Gettig, R.R., Burand, J.P., Carmichael, L.E., Wood, H.A., and Parrish, C.R. 1992. Canine parvovirus empty capsids produced by expression in a baculovirus vector: use in analysis of viral properties and immunization of dogs. *J Gen Virol.* 73:369-374.

Samols, D., Thornton, C.G., Murtif, V.L., Kumar, G.K., Haase, F.C., and Wood, H.G. 1988. Evolutionary conservation among biotin enzymes. *J Biol. Chem.* 263:6461-6464. Review.

Schatz, P.J. 1993. Use of peptide libraries to map the substrate specificity of a peptide-modifying enzyme: a 13 residue consensus peptide specifies biotinylation in *Escherichia coli*. *Biotechnology.* 11:1138-1143.

Sheff, D.R., Daro, E.A., Hull, M., and Mellman, I. 1999. The receptor recycling pathway contains two distinct populations of early endosomes with different sorting functions. *J Cell Biol.* 145:123-139.

Suikkanen, S., Sääjärvi, K., Hirsimäki, J., Välilehto, O., Reunanen, H., Vihinen-Ranta, M., and Vuento, M. 2002. Role of recycling endosomes and lysosomes in dynein-dependent entry of canine parvovirus. *J Virol.* 76:4401-4011.

Suikkanen, S., Antila, M., Jaatinen, A., Vihinen-Ranta, M., and Vuento, M. 2003I. Release of canine parvovirus from endocytic vesicles. *Virology.* 316:267-280.

Suikkanen, S., Aaltonen, T., Nevalainen, M., Välilehto, O., Lindholm, L., Vuento, M., and Vihinen-Ranta, M. 2003II. Exploitation of microtubule cytoskeleton and dynein during parvoviral traffic toward the nucleus. *J Virol.* 77:10270-10279.

Tattersall, P. 1972. Replication of the parvovirus MVM. I. Dependence of virus multiplication and plaque formation on cell growth. *J Virol.* 10:586-590.

Tissot, G., Douce, R., and Alban, C. 1997. Evidence for multiple forms of biotin holocarboxylase synthetase in pea (*Pisum sativum*) and in Arabidopsis thaliana: subcellular fractionation studies and isolation of a cDNA clone. *Biochem. J.* 323:179-188.

Trischler, M., Stoorvogel, W., and Ullrich, O. 1999. Biochemical analysis of distinct Rab5- and Rab11-positive endosomes along the transferrin pathway. *J Cell Sci.* 112:4773-4783.

Trowbridge, I.S., and Omary, M.B. 1981. Human cell surface glycoprotein related to cell proliferation is the receptor for transferrin. *Proc. Natl. Acad. Sci.* 78:3039-3043.

Truyen, U., and Parrish, C.R. 1992. Canine and feline host ranges of canine parvovirus and feline panleukopenia virus: distinct host cell tropisms of each virus in vitro and in vivo. *J Virol.* 66:5399-5408.

Tsao, J., Chapman, M.S, Agbandje, M., Keller, W., Smith, K., Wu, H., Luo, M., Smith, T.J., Rossmann, M.G, Compans, R.W, and Parrish, C.R. 1991. The three-dimensional structure of canine parvovirus and its functional implications. *Science.* 251:1456-1464.

Vihinen-Ranta, M., Kakkola, L., Kalela, A., Vilja, P., and Vuento, M. 1997. Characterization of a nuclear localization signal of canine parvovirus capsid proteins. *Eur. J Biochem.* 250:389-394.

Vihinen-Ranta, M., Kalela, A., Mäkinen, P., Kakkola, L., Marjomäki, V., and Vuento, M. 1998. Intracellular route of canine parvovirus entry. *J Virol.* 72:802-806.

Vihinen-Ranta, M., Yuan, W., and Parrish, C.R. 2000. Cytoplasmic trafficking of the canine parvovirus capsid and its role in infection and nuclear transport. *J Virol.* 74:4853-4859.

Vihinen-Ranta, M., Suikkanen, S., and Parrish, C.R. 2004. Pathways of cell infection by parvoviruses and adeno-associated viruses. *J Virol.* 78:6709-6714. Review.

Vogt, T.M., Blackwell, A.D., Giannetti, A.M., Björkman, P.J., and Enns, C.A. 2003. Heterotypic interactions between transferrin receptor and transferrin receptor 2. *Blood.* 101:2008-2014.

Watson, A., Wu, X., and Bruchez, M. 2003. Lighting up cells with quantum dots. *Biotechniques.* 34:296-300, 302-303. Review.

Weichert, W.S., Parker, J.S., Wahid, A.T., Chang, S.F., Meier, E., and Parrish, C.R. 1998. Assaying for structural variation in the parvovirus capsid and its role in infection. *Virology.* 250:106-117.

Weissman, A.M., Klausner, R.D., Rao, K., and Harford, J.B. 1986. Exposure of K562 cells to anti-receptor monoclonal antibody OKT9 results in rapid redistribution and enhanced degradation of the transferrin receptor. *J Cell Biol*. 102:951-958.

Wilson, K.P., Shewchuk, L.M., Brennan, R.G., Otsuka, A.J., and Matthews, B.W. 1992. *Escherichia coli* biotin holoenzyme synthetase/bio repressor crystal structure delineates the biotin- and DNA-binding domains. *Proc. Natl. Acad. Sci.* 89:9257-9261.

Xie, Q., and Chapman, M.S. 1996. Canine parvovirus capsid structure, analyzed at 2.9 Å resolution. *J Mol. Biol.* 264:497-520.

Xu, Y., Nenortas, E., and Beckett, D. 1995. Evidence for distinct ligand-bound conformational states of the multifunctional *Escherichia coli* repressor of biotin biosynthesis. *Biochemistry.* 34:16624-16631.

Xu, Y., and Beckett, D. 1996. Evidence for interdomain interaction in the *Escherichia coli* repressor of biotin biosynthesis from studies of an N-terminal domain deletion mutant. *Biochemistry.* 35:1783-1792.

Zadori, Z., Szelei, J., Lacoste, M.C., Li, Y., Gariepy, S., Raymond, P., Allaire, M., Nabi, I.R., and Tijssen, P. 2001. A viral phospholipase A2 is required for parvovirus infectivity. *Dev. Cell.* 1:291-302.

Zahringer, J., Baliga, B.S., Munro, H.N. 1976. Novel mechanism for translational control in regulation of ferritin synthesis by iron. *Proc. Natl. Acad. Sci.* 73:857-861.

Zimmer, M. 2002. Green fluorescent protein (GFP): applications, structure, and related photophysical behavior. *Chem. Rev.* 102:759-781. Review.